

AD-A255 239



①

III-V SEMICONDUCTOR QUANTUM WELL LASERS AND  
RELATED OPTOELECTRONIC DEVICES (ON SILICON)

FINAL REPORT

(and beginning of:

OXIDE-DEFINED SEMICONDUCTOR QUANTUM WELL LASERS AND  
OPTOELECTRONIC DEVICES: Al-BASED III-V NATIVE OXIDES)

N. Holonyak, Jr./K. C. Hsieh/G. E. Stillman  
May, 1992

U.S. ARMY RESEARCH OFFICE  
DAAL 03-89-K-0008

Department of Electrical and Computer Engineering  
University of Illinois at Urbana-Champaign  
Urbana, IL 61801

APPROVED FOR PUBLIC RELEASE;  
DISTRIBUTION UNLIMITED

DTIC  
SEP 11 1992  
C

92-24958



37p95

THE VIEW, OPINIONS, AND/OR FINDINGS CONTAINED IN THIS REPORT  
ARE THOSE OF THE AUTHOR(S) AND SHOULD NOT BE CONSTRUED AS  
AN OFFICIAL DEPARTMENT OF THE ARMY POSITION, POLICY, OR  
DECISION, UNLESS SO DESIGNATED BY OTHER DOCUMENTATION.

## TABLE OF CONTENTS

	Page
I. INTRODUCTION.....	2
II. Al-BASED III-V OXIDES ON QUANTUM WELL HETEROSTRUCTURES.....	3
III. QUANTUM WELL LASERS DEFINED BY Al-BEARING III-V NATIVE OXIDES.....	4
IV. NATIVE-OXIDE-DEFINED DEVICE GEOMETRIES (NEW DEVICES).....	5
V. MISCELLANEOUS.....	7
VI. CONTRIBUTORS.....	8
REFERENCES.....	11

A-1

## I. INTRODUCTION

Since the beginning of this project (10+ years ago) we have been concerned with quantum well heterostructures (QWHs) and their use in advanced forms of lasers, light emitting diodes (LEDs), and more generally in optoelectronics. This has led us into a wide range of studies and discoveries, including the commercially important process (patented) of impurity-induced layer disordering (which can be employed to change a QWH, in whatever pattern desired, from QW lower gap to bulk-crystal higher energy band gap). In the course of a long series of investigations on GaAs-Al<sub>x</sub>Ga<sub>1-x</sub>As-AlAs QWHs, some with thick AlAs cladding layers ( $\geq 0.1 \mu\text{m}$ ), we have observed and tracked (0  $\rightarrow$  10 years) the atmospheric hydrolyzation of high Al composition Al<sub>x</sub>Ga<sub>1-x</sub>As.<sup>1,2</sup> By attempting to accelerate AlAs and Al<sub>x</sub>Ga<sub>1-x</sub>As hydrolyzation with higher humidities and higher temperatures, e.g., via H<sub>2</sub>O vapor ( $\sim 95^\circ\text{C}$ ) in an N<sub>2</sub> carrier gas and sample temperatures  $\geq 400^\circ\text{C}$ , we have crossed over from lesser (or poorer) oxide phases to higher (or better) oxide phases.<sup>3</sup> Preferably these are oxides not involving Al(OH)<sub>3</sub> (gibbsite) but AlO(OH) (diaspore) or even  $\gamma$  Al<sub>2</sub>O<sub>3</sub>. These Al-bearing oxides prove to be stable and useful and, in essence, have permitted us to introduce a successful new native-oxide technology into III-V heterostructure electronics. This technology employs as the source for the formation of the oxide layers (derived by "wet" oxidation,  $\geq 400^\circ\text{C}$ ) Al<sub>x</sub>Ga<sub>1-x</sub>As cladding layers, or, in fact, other Al-rich III-V cladding layers (e.g., InGaAlP, InAlAs, etc.). The key to the success of these native oxides in device applications is the presence of the Al component, which, unlike Ga, yields useful stable oxides (via "wet" oxidation at higher temperatures,  $\geq 400^\circ\text{C}$ ) and not fragile hydrolyzation

products, essentially "debris". This new work of the last two years, which brings true integrated circuit (IC) technology into III-V heterostructure device electronics, is described in the publications listed here as Refs. 1-20, as well as in two patent applications (Refs. 21 and 22).

## II. Al-BASED III-V OXIDES ON QUANTUM WELL HETEROSTRUCTURES

The AlAs and  $\text{Al}_x\text{Ga}_{1-x}\text{As}$  hydrolyzation (destructive) that initiated this new area of work ~ 2 years ago is described in Refs. 1 and 2, and then, in total contrast, in Ref. 3 we describe the "wet" oxidation formation ( $\geq 400^\circ\text{C}$ ) of stable  $\text{Al}_x\text{Ga}_{1-x}\text{As}$  native oxides. Reference 3 is of special interest because it shows the difference between "wet" oxidation of an AlAs-GaAs superlattice (anisotropic oxidation) and similar oxidation of its disordered homogeneous  $\text{Al}_x\text{Ga}_{1-x}\text{As}$  alloy (isotropic). These studies continue because of fundamental and device reasons.

We have established that these new "wet"-oxidation Al-bearing III-V native oxides are capable of surface protection (Ref. 7), differ in formation rate for Fermi level reasons in p and n material (Ref. 18), and are effective in impurity-diffusion masking (Refs. 6 and 11). Also, the III-V native oxide can be used in delineating device geometries in conjunction with layer disordering (Ref. 8). That is, the oxide and layer disordering technologies are compatible (complementary) technologies, and can be combined to advantage.

One of the main problems of the Al-bearing III-V native oxides, and less reported, is that dealing with the oxide-semiconductor interface and charged species (ions, defects, etc.) at the interface. Because of their importance in field effect devices, these problems (along with anisotropic oxidation)

continue to be worked on, as well as, of course, the basic III-V native oxide properties.

### III. QUANTUM WELL LASERS DEFINED BY Al-BEARING III-V NATIVE OXIDES

We recognized from the outset when we transformed the problem of AlAs or  $\text{Al}_x\text{Ga}_{1-x}\text{As}$  cladding-layer hydrolyzation into the advantageous circumstance of generation of stable III-V native oxides on QWHs that a particularly useful new device technology, an integrated-circuits (IC) style technology, was the result. We have demonstrated the usefulness, as well as importance, of the native oxide technology first on more or less simple single-stripe gain-guided lasers (Ref. 4) and then coupled-stripe gain-guided  $\text{Al}_x\text{Ga}_{1-x}\text{As}$ -GaAs QWH lasers (Ref. 5). The latter has been extended to strained-layer  $\text{Al}_y\text{Ga}_{1-y}\text{As}$ -GaAs- $\text{In}_x\text{Ga}_{1-x}\text{As}$  QWHs (Ref. 9). Because Al-bearing III-V native oxides can be made thick ( $> 0.1 \mu\text{m}$ ) in addition to just thin ( $\leq 0.1 \mu\text{m}$ ), and are well matched on their parent crystal, they can be used to advantage to make sophisticated thick-oxide single-stripe planar index-guided lasers (Ref. 12), not to mention coupled-stripe planar QWH lasers (Ref. 15).

Any QWH system (high or low gap) that can be grown on GaAs can be provided with an  $\text{Al}_x\text{Ga}_{1-x}\text{As}$  surface oxidation layer for use in forming the cladding native oxide (for use in defining or protecting devices). An example (Ref. 16) is the  $\text{Al}_x\text{Ga}_{1-x}\text{As-In}_{0.5}(\text{Al}_y\text{Ga}_{1-y})_{0.5}\text{P-In}_{0.5}(\text{Al}_z\text{Ga}_{1-z})_{0.5}\text{P}$  high gap system (visible spectrum) grown on GaAs, which demonstrates the point that an  $\text{Al}_x\text{Ga}_{1-x}\text{As}$  oxidation layer can be employed quite universally in various III-V systems. In the case of the high gap  $\text{In}(\text{AlGa})\text{P}$  system, the  $\text{In}_{0.5}(\text{Al}_y\text{Ga}_{1-y})_{0.5}\text{P}$  upper cladding layer itself can be employed as the

oxidation layer if the Al composition ( $y$ ) is sufficiently high. This is demonstrated by the native-oxide-defined single-stripe and coupled-stripe lasers of Refs. 10 and 14. The In(AlGa)P quaternary system is important and continues to be part of our further studies.

#### IV. NATIVE-OXIDE-DEFINED DEVICE GEOMETRIES (NEW DEVICES)

Clearly the III-V native-oxide technology described here, i.e., "wet" oxidation of Al-bearing III-V cladding layers, allows realization of much more complicated device geometries than those of the simple single-stripe and coupled-stripe lasers we have demonstrated in our initial work. A thick planar oxide technology that can be used in index guiding has obvious usefulness in constructing optical waveguides with more extreme (sharper) curvature than has been realized with previous planar technologies (e.g., by impurity induced layer disordering). As an example, which is a form of existence proof, Ref. 17 describes planar ring laser diodes we have constructed via "wet" oxidation of the upper  $\text{Al}_x\text{Ga}_{1-x}\text{As}$  cladding layer of  $\text{Al}_x\text{Ga}_{1-x}\text{As-GaAs}$  QWHs. These devices are of intrinsic interest because of the nature of ring lasers themselves, but also are of further interest for study of the various parameters controlling wave bending and confinement.

An Al-based III-V native-oxide technology such as now dominates our work provides special advantage in convenient realization of complicated device geometries. One of the first that we have considered is what appears externally to be an ordinary single-stripe QWH laser but which internally is a linear array of small rectangular coupled cavities (Ref. 13). Utilizing the Al-based III-V native-oxide technology, we realize (simply) the coupled-cavity

linear array of Ref. 13 by employing in the device processing the usual single-stripe photomask pattern along with a second photomask of uniformly spaced lines turned at right angles. This simply and conveniently realized planar linear-array stripe-geometry laser exceeds in its complexity by far a so-called cleaved-coupled-cavity laser.

As readily as we can realize the simple linear array described in Ref. 13, we can fabricate much more complicated two-dimensional (2-D) planar arrays. This obviously opens up an entire new field of study. An example, with major consequences, is that of simply coupling side by side (via the "wet" oxidation native-oxide technology) two of the linear arrays of Ref. 13. The resulting elementary 2-D array, which superficially is in the form of a twin stripe laser, becomes a two terminal, or if desired, three or more terminal photonic switching device (Ref. 20). The laser light versus current characteristic (L-I characteristic), which in a typical laser diode exhibits (until heating) a monotonic increase in light output with increase in current, in the case of the 2-D twin linear array exhibits ON-OFF switching behavior. This has not been achieved previously (for 29+ years), i.e., self-switching of a semiconductor laser from spontaneous to stimulated to spontaneous to stimulated emission with increasing current. We note that in the two-terminal device (a QWH laser) of Ref. 20 the device current is partitioned among many identical elements, which themselves are interconnected with the photons they generate. A uniform array tends to exhibit "pass bands" and "stop bands", and tends to support stimulated emission ON-resonance and spontaneous emission (and switching) OFF-resonance. We note that because of how we have partitioned the current among the elements of the array, the laser



(unlike ordinary semiconductor lasers) tends to exhibit inhomogeneous broadening. We can, and have, made a fundamental change in the semiconductor laser.

In the interest of brevity and also because of the early state of this work, we do not wish to say much more except to mention that, the III-V native-oxide IC technology we have disclosed, and the exploratory oxide-defined array devices of Refs. 13 and 20, are the basis for an entire new class of electronic-photonic laser switching elements. It is hard to estimate the importance of these developments, which we intend to pursue further in our study of III-V native oxides and their use in QWH devices.

#### V. MISCELLANEOUS

We mention that on account of our broad general background in III-V semiconductor and quantum well heterostructure research, we have made contributions to other related problems (Refs. 23 and 24). Also, we have presented an invited talk (recorded and to be made available by APS) in the commemorative symposium devoted to John Bardeen at the March Meeting (Indianapolis) of the American Physical Society (Ref. 25).

## VI. CONTRIBUTORS

The principal investigators contributing to various parts of the work reported here are:

- 1) N. Holonyak, Jr.
- 2) K. C. Hsieh
- 3) G. E. Stillman

(This report and proposal for further work has been prepared by N. Holonyak, Jr.) Note that some of the work we have reported here has been done in cooperation with Burnham's group at Amoco (Naperville, Illinois) and with Craford's group at Hewlett-Packard (San Jose). In other words, the Al-based III-V native oxide technology we have disclosed here (which originated in Urbana in this project) has already involved and gotten the attention of American industry. Most recently we have used the oxide technology on Xerox In(AlGa)P crystals (Bour, et al.) and have fabricated high performance (state-of-the-art) visible-spectrum (660 nm) lasers with so-called "window" outputs on the cavity ends.

The graduate students either receiving direct project support or otherwise contributing to various portions of the work reported here are:

- 1) J. M. Dallesasse, Ph.D. completed. (Now at Amoco, Naperville, Illinois.)
- 2) D. C. Hall, Ph. D. completed. (Now at Naval Research Laboratory.)

- 3) F. A. Kish, Ph.D. Student. (A.T.&T. Fellowship; Ph.D. research almost completed, Spring, 1992.)
- 4) A. R. Sugg, Ph.D. Student. (Ph.D. preliminary examination completed, Spring, 1991.)
- 5) G. E. Höfler, Ph.D. student (Hsieh advisor). (Ph.D. preliminary examination completed, Fall, 1991).
- 6) S. J. Caracci, Ph. D. Student. (Air Force "Palace Nights" Program; Ph.D. preliminary examination completed, Spring, 1992).
- 7) T. A. Richard, Ph.D. Student. (Ph.D. qualifying examination completed; course work completed, Spring, 1992.)
- 8) N. El-Zein, Ph.D. Student. (Ph.D. qualifying examination completed; course work completed, Spring, 1992.)
- 9) S. A. Maranowski, Ph.D. student (Ph.D. qualifying examination completed, Spring, 1991.)
- 10) M. J. Ries, Ph.D. Student. (Ph.D. qualifying examination completed, Fall, 1991.)
- 11) E. Chen, Ph.D. student. (Ph.D. qualifying examination completed, Fall, 1991.)
- 12) M. Krames, Ph.D. Student (Ph.D. qualifying examination completed, Fall, 1991).

Note that some of the graduate students making contributions to this work have received support from other projects or have received fellowship support. We mention that the National Science Foundation Engineering Research Center has supported much of our MOCVD crystal growth (EMCORE reactor), and our NSF MRL has supported our TEM and SIMS analyses, which are spread throughout much of the work reported here.

We note that patent protection on the  $\text{Al}_x\text{Ga}_{1-x}\text{As}$  ( $x \geq 0.7$ ) native oxide technology we have introduced is being handled for the University of Illinois by Research Corporation Technology, and in one case by the University directly. Two patent applications (Refs. 21 and 22) have been filed on our work on Al-based III-V native oxides.

Finally, on November 13, 1990 N. Holonyak, Jr. was awarded the National Medal of Science at the White House by President George Bush. In May 1992 he received the Optical Society of America Charles Hard Townes Award, and on 20 June 1992 is to receive an honorary doctor of science degree from Northwestern University.

## REFERENCES

1. J. M. Dallesasse, P. Gavrilovic, N. Holonyak, Jr., R. W. Kaliski, D. W. Nam, E. J. Vesely, and R. D. Burnham, "Stability of AlAs in  $\text{Al}_x\text{Ga}_{1-x}\text{As}$ -AlAs-GaAs Quantum Well Heterostructures," Appl. Phys. Lett. 56, 2436-2438 (11 June 1990).
2. J. M. Dallesasse, N. El-Zein, N. Holonyak, Jr., K. C. Hsieh, R. D. Burnham, and R. D. Dupuis, "Environmental Degradation of  $\text{Al}_x\text{Ga}_{1-x}\text{As}$ -GaAs Quantum-Well Heterostructures," J. Appl. Phys. 68, 2235-2238 (1 September 1990).
3. J. M. Dallesasse, N. Holonyak, Jr., A. R. Sugg, T. A. Richard, and N. El-Zein, "Hydrolyzation-Oxidation of  $\text{Al}_x\text{Ga}_{1-x}\text{As}$ -AlAs-GaAs Quantum Well Heterostructures and Superlattices," Appl. Phys. Lett. 57, 2844-2846 (24 December 1990).
4. J. M. Dallesasse and N. Holonyak, Jr., "Native-Oxide Stripe-Geometry  $\text{Al}_x\text{Ga}_{1-x}\text{As}$ -GaAs Quantum Well Heterostructure Lasers," Appl. Phys. Lett. 58, 394-396 (28 January 1991).
5. J. M. Dallesasse, N. Holonyak, Jr., D. C. Hall, N. El-Zein, A. R. Sugg, S. C. Smith, and R. D. Burnham, "Native-Oxide-Defined Coupled-Stripe  $\text{Al}_x\text{Ga}_{1-x}\text{As}$ -GaAs Quantum-Well Heterostructure Lasers," Appl. Phys. Lett. 58, 834-836 (25 February 1991).
6. J. M. Dallesasse, N. Holonyak, Jr., N. El-Zein, T. A. Richard, F. A. Kish, A. R. Sugg, R. D. Burnham, and S. C. Smith, "Native-Oxide Masked Impurity-Induced Layer Disordering of  $\text{Al}_x\text{Ga}_{1-x}\text{As}$  Quantum Well Heterostructures," Appl. Phys. Lett. 58, 974-976 (4 March 1991).
7. A. R. Sugg, N. Holonyak, Jr., J. E. Baker, F. A. Kish, and J. M. Dallesasse, "Native Oxide Stabilization of AlAs-GaAs Heterostructures," Appl. Phys. Lett. 58, 1199-1201 (11 March 1991).
8. F. A. Kish, S. J. Caracci, N. Holonyak, Jr., J. M. Dallesasse, G. E. Höfler, R. D. Burnham, and S. C. Smith, "Low-Threshold Disorder-Defined Native-Oxide-Delineated Buried-Heterostructure  $\text{Al}_x\text{Ga}_{1-x}\text{As}$ -GaAs Quantum Well Lasers," Appl. Phys. Lett. 58, 1765-1767 (22 April 1991).
9. T. A. Richard, F. A. Kish, N. Holonyak, Jr., J. M. Dallesasse, K. C. Hsieh, M. J. Ries, P. Gavrilovic, K. Meehan, and J. E. Williams, "Native-Oxide Coupled-Stripe  $\text{Al}_y\text{Ga}_{1-y}\text{As}$ -GaAs- $\text{In}_x\text{Ga}_{1-x}\text{As}$  Quantum Well Heterostructure Lasers," Appl. Phys. Lett. 58, 2390-2392 (27 May 1991).
10. F. A. Kish, S. J. Caracci, N. Holonyak, Jr., J. M. Dallesasse, A. R. Sugg, R. M. Fletcher, C. P. Kuo, T. D. Osentowski, and M. G. Craford, "Native-Oxide Stripe-Geometry  $\text{In}_{0.5}(\text{Al}_x\text{Ga}_{1-x})_{0.5}\text{P}$ - $\text{In}_{0.5}\text{Ga}_{0.5}\text{P}$  Heterostructure Laser Diodes," Appl. Phys. Lett. 59, 354-356 (22 July 1991).

11. N. El-Zein, N. Holonyak, Jr., F. A. Kish, A. R. Sugg, T. A. Richard, J. M. Dallesasse, S. C. Smith, and R. D. Burnham, "Native-Oxide-Masked Si Impurity-Induced Layer Disordering of  $\text{Al}_x\text{Ga}_{1-x}\text{As}-\text{Al}_y\text{Ga}_{1-y}\text{As}-\text{Al}_z\text{Ga}_{1-z}\text{As}$  Quantum Well Heterostructures," J. Appl. Phys. 70, 2031-2034 (15 Aug 1991).
12. F. A. Kish, S. J. Caracci, N. Holonyak, Jr., J. M. Dallesasse, K. C. Hsieh, M. J. Ries, S. C. Smith, and R. D. Burnham, "Planar Native-Oxide Index-Guided  $\text{Al}_x\text{Ga}_{1-x}\text{As}-\text{GaAs}$  Quantum Well Heterostructure Lasers," Appl. Phys. Lett. 59, 1755-1757 (30 Sept 1991).
13. N. El-Zein, F. A. Kish, N. Holonyak, Jr., A. R. Sugg, M. J. Ries, S. C. Smith, J. M. Dallesasse, and R. D. Burnham, "Native-Oxide Coupled-Cavity  $\text{Al}_x\text{Ga}_{1-x}\text{As}-\text{GaAs}$  Quantum Well Heterostructure Laser Diodes," Appl. Phys. Lett. 59, 2838-2840 (25 Nov 1991).
14. F. A. Kish, S. J. Caracci, N. Holonyak, Jr., S. A. Maranowski, J. M. Dallesasse, R. D. Burnham, and S. C. Smith, "Visible Spectrum Native-Oxide Coupled-Stripe  $\text{In}_{0.5}(\text{Al}_x\text{Ga}_{1-x})_{0.5}\text{P}-\text{In}_{0.5}\text{Ga}_{0.5}\text{P}$  Quantum Well Heterostructure Laser Arrays," Appl. Phys. Lett. 59, 2883-2885 (25 Nov 1991).
15. F. A. Kish, S. J. Caracci, N. Holonyak, Jr., P. Gavrilovic, K. Meehan, and J. E. Williams, "Coupled-Stripe In-Phase Operation of Planar Native-Oxide Index-Guided  $\text{Al}_y\text{Ga}_{1-y}\text{As}-\text{GaAs}-\text{In}_x\text{Ga}_{1-x}\text{As}$  Quantum Well Heterostructure Laser Arrays," Appl. Phys. Lett. 60, 71-73 (6 Jan 1992).
16. F. A. Kish, S. J. Caracci, S. A. Maranowski, N. Holonyak, Jr., K. C. Hsieh, C. P. Kuo, R. M. Fletcher, T. D. Osentowski, and M. G. Craford, "Planar Native-Oxide Buried-Mesa  $\text{Al}_x\text{Ga}_{1-x}\text{As}-\text{In}_{0.5}(\text{Al}_y\text{Ga}_{1-y})_{0.5}\text{P}-\text{In}_{0.5}(\text{Al}_z\text{Ga}_{1-z})_{0.5}\text{P}$  Visible-Spectrum Laser Diodes," J. Appl. Phys. 71, 2521-2525 (15 March 1992).
17. F. A. Kish, S. J. Caracci, S. A. Maranowski, N. Holonyak, Jr., S. C. Smith, and R. D. Burnham, "Planar Native-Oxide  $\text{Al}_x\text{Ga}_{1-x}\text{As}-\text{GaAs}$  Quantum Well Heterostructure Ring Laser Diodes," Appl. Phys. Lett. 60, 1582-1584 (30 March 1992).
18. F. A. Kish, S. A. Maranowski, G. E. Höfler, N. Holonyak, Jr., S. J. Caracci, J. M. Dallesasse, and K. C. Hsieh, "Dependence of Doping Type (p/n) of the Water Vapor Oxidation of High-Gap  $\text{Al}_x\text{Ga}_{1-x}\text{As}$ ," Appl. Phys. Lett. 60, (22 June 1992).
19. S. J. Caracci, F. A. Kish, N. Holonyak, Jr., S. A. Maranowski, S. C. Smith and R. D. Burnham, "High-Performance Planar Native-Oxide Buried-Mesa Index-Guided  $\text{AlGaAs}-\text{GaAs}$  Quantum Well Heterostructure Lasers" Appl. Phys. Lett. 61, (20 July, 1992).
20. N. El-Zein, N. Holonyak, Jr., F. A. Kish, S. C. Smith, J. M. Dallesasse, and R. D. Burnham, "Resonance and Switching in a Native-Oxide-Defined  $\text{Al}_x\text{Ga}_{1-x}\text{As}-\text{GaAs}$  Quantum Well Heterostructure Laser Array,"

21. Nick Holonyak, Jr. and John M. Dallesasse, "AlGaAs NATIVE OXIDE" (Filed 31 December 1990), not yet issued.
22. Nick Holonyak, Jr., F. A. Kish, and S. J. Caracci, "SEMICONDUCTOR DEVICES AND TECHNIQUES FOR CONTROLLED OPTICAL CONFINEMENT," (Filed March 30, 1992), not yet issued.
23. C. H. Wu, K. C. Hsieh, G. E. Höler, N. El-Zein, and N. Holonyak, Jr., "Diffusion of Manganese in GaAs and its Effect on Layer Disordering in  $\text{Al}_x\text{Ga}_{1-x}\text{As-GaAs}$  Superlattices," Appl. Phys. Lett. 59, 1224-1226 (2 Sept 1991).
24. G. E. Höfler, H. J. Höfler, N. Holonyak, Jr., and K. C. Hsieh, "Effect of Annealing Temperature on Hole Concentration and Lattice Relaxation of Carbon Doped GaAs and  $\text{Al}_x\text{Ga}_{1-x}\text{As}$ ."
25. N. Holonyak, Jr., "John Bardeen and the Point Contact Transistor," Physics Today, Vol. 45 (#4), 36-43 (April, 1992).

# Stability of AlAs in $\text{Al}_x\text{Ga}_{1-x}\text{As}$ -AlAs-GaAs quantum well heterostructures

J. M. Dallesasse, P. Gavrilovic,<sup>a)</sup> N. Holonyak, Jr., R. W. Kaliski,<sup>b)</sup> D. W. Nam,<sup>c)</sup> and E. J. Vesely<sup>d)</sup>

*Electrical Engineering Research Laboratory, Center for Compound Semiconductor Microelectronics, and Materials Research Laboratory, University of Illinois at Urbana-Champaign, Urbana, Illinois 61801*

R. D. Burnham

*Amoco Technology Company, Amoco Research Center, Naperville, Illinois 60566*

(Received 12 January 1990; accepted for publication 3 April 1990)

Data are presented on the long-term ( $\geq 8$  yr) degradation of  $\text{Al}_x\text{Ga}_{1-x}\text{As}$ -AlAs-GaAs quantum well heterostructure material because of the instability of underlying (internal) AlAs layers. Material containing thicker ( $> 0.4 \mu\text{m}$ ) AlAs "buried" layers (confining layers) is found to be much less stable than material containing thinner ( $\leq 200 \text{ \AA}$ ) AlAs layers. Hydrolysis of the AlAs layers because of cleaved edges and pinholes in the cap layers leads to the deterioration.

Since the introduction of AlAs barrier layers in  $\text{Al}_x\text{Ga}_{1-x}\text{As}$ -GaAs quantum well heterostructures (QWHs) to suppress the effects of alloy clustering,<sup>1</sup> the use of AlAs layers in QWHs has become quite common in lasers and other devices. It is of interest that almost from the beginning of extensive study of III-V compounds the binary Al-bearing III-V's have been listed as unstable.<sup>2</sup> In early work on high-performance  $\text{Al}_x\text{Ga}_{1-x}\text{As}$ -GaAs solar cells, AlAs layers employed as window layers have been found to be unstable when exposed to air.<sup>3,4</sup> In order to circumvent this problem, AlAs layers have either been passivated using anodization,<sup>3</sup> or have been replaced by high-composition ( $x \sim 0.8$ )  $\text{Al}_x\text{Ga}_{1-x}\text{As}$  layers.<sup>4</sup> In QWHs they are, of course, "buried" in the layered structure. As is well known<sup>2</sup> the instability of AlAs is due to the extremely reactive nature of the Al, particularly in a moist environment. Because of this behavior, an important consideration for the reliable operation of QWH lasers, as well as other QWH devices, is the stability of the AlAs layers if they are employed in the QWH. In this letter data are presented on the degradation of AlAs in  $\text{Al}_x\text{Ga}_{1-x}\text{As}$ -AlAs-GaAs QWHs and superlattices (SLs). Thicker ( $> 0.4 \mu\text{m}$ ) AlAs layers that are exposed to the environment through "pinholes" in encapsulating layers or at cleaved edges are found to decompose, resulting in a slow destruction of the QWH material. Thinner AlAs layers ( $< 200 \text{ \AA}$ ) contained within a SL structure are found to have increased stability.

The crystals used in this experiment are grown by metalorganic chemical vapor deposition (MOCVD) on {100} *n*-type GaAs substrates.<sup>5</sup> In Fig. 1(b) a scanning electron microscope (SEM) photomicrograph of the cross section of the primary QWH material used in this experiment is shown. Growth begins with a thick *n*-type GaAs buffer layer and then an  $\text{Al}_{0.75}\text{Ga}_{0.25}\text{As}$  layer ( $\sim 0.8 \mu\text{m}$ ). This is followed by a  $\sim 0.4\text{-}\mu\text{m}$ -thick *n*-type AlAs lower confining layer. Next is the symmetrical active region of the QWH which

consists of a  $\sim 150 \text{ \AA}$  GaAs quantum well (QW) between two  $\sim 600 \text{ \AA}$   $\text{Al}_{0.2}\text{Ga}_{0.8}\text{As}$  waveguide (WG) layers. Then a thick ( $\sim 0.5 \mu\text{m}$ ) AlAs *p*-type upper confining layer is grown, followed by the growth of a  $\sim 0.4 \mu\text{m}$  *p*-type  $\text{Al}_{0.75}\text{Ga}_{0.25}\text{As}$  layer. The entire structure is capped by a heavily doped *p*-type GaAs cap layer ( $\sim 0.6 \mu\text{m}$ ). The 40-period comparison SL sample is grown similarly by MOCVD but with  $150 \text{ \AA}$  AlAs barriers and  $45 \text{ \AA}$  GaAs wells.

The *p-n* QWH crystal of main issue here dates back to April, 1982. At the time of its growth unmounted probe tested laser diodes exhibited (300 K) pulsed threshold current densities of  $3000 \text{ A/cm}^2$ . This indicates fair quality crystal. The as-grown crystal was observed (by optical microscopy) to be free of any obvious defects. The wafer was then maintained under normal room environmental conditions. With the passage of time, atmospheric water vapor reacts with the buried AlAs layers, possibly forming  $\text{Al}_2\text{O}_3$ ,  $\text{Al}_2\text{O}_3 \cdot \text{H}_2\text{O}$ ,  $\text{Al}_2\text{O}_3 \cdot 3\text{H}_2\text{O}$ ,  $\text{AlAs} \cdot 8\text{H}_2\text{O}$ ,  $\text{AlO}(\text{OH})$ , or  $\text{Al}(\text{OH})_3$ . This occurs via crystal edges and pinholes in the GaAs-Al $_x\text{Ga}_{1-x}\text{As}$  encapsulating layers, thus leading to slow decomposition of the QWH material. Two examples of the destructive reactions that can occur are

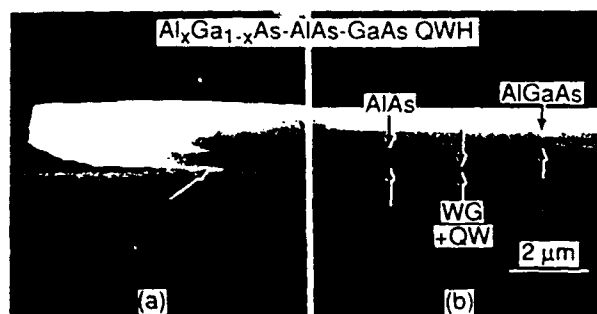


FIG. 1. Scanning electron microscope (SEM) photomicrograph of the cross section of an  $\text{Al}_x\text{Ga}_{1-x}\text{As}$ -AlAs-GaAs QWH grown in 1982 that, because of thick ( $\geq 0.4 \mu\text{m}$ ) "buried" AlAs confining layers and cleaved edges and pinholes, hydrolyzes and deteriorates. The arrow in (a) marks the boundary between hydrolyzed AlAs and AlAs that is unreacted. Panel (b) shows the layer structure of the as-grown QWH material in an area unaffected by the hydrolysis.

<sup>a)</sup> Now at Polaroid (Polaroid Corp., 21 Osborn St., Cambridge, MA 02139).

<sup>b)</sup> Now at Amoco (Amoco Research Center, Naperville, Illinois 60566).

<sup>c)</sup> Kodak Doctoral Fellow.

<sup>d)</sup> National Science Foundation Doctoral Fellow.



# Environmental degradation of $\text{Al}_x\text{Ga}_{1-x}\text{As}$ -GaAs quantum-well heterostructures

J. M. Dallesasse, N. El-Zein, N. Holonyak, Jr., and K. C. Hsieh

*Electrical Engineering Research Laboratory, Center for Compound Semiconductor Microelectronics, and Materials Research Laboratory, University of Illinois at Urbana-Champaign, Urbana, Illinois 61801*

R. D. Burnham

*Amoco Research and Development, Naperville, Illinois 60566*

R. D. Dupuis

*University of Texas at Austin, Austin, Texas 78712*

(Received 5 April 1990; accepted for publication 14 May 1990)

Data describing the deterioration of  $\text{Al}_x\text{Ga}_{1-x}\text{As}$ -GaAs heterostructures in long-term exposure (2–12 years) to normal room environmental conditions ( $\sim 20$ – $25^\circ\text{C}$ , varying humidity) are presented. Optical microscopy, scanning electron microscopy, transmission electron microscopy, and electron dispersion x-ray spectroscopy are used to examine  $\text{Al}_x\text{Ga}_{1-x}\text{As}$ -GaAs quantum-well heterostructure material that has hydrolyzed at cleaved edges, cracks, and fissures, and at pinholes in cap layers. The hydrolysis is found to be significant for thicker ( $> 0.1\ \mu\text{m}$ )  $\text{Al}_x\text{Ga}_{1-x}\text{As}$  layers of higher composition ( $x > 0.85$ ).

## I. INTRODUCTION

An important question in the long-term stability, and thus reliability, of  $\text{Al}_x\text{Ga}_{1-x}\text{As}$ -GaAs quantum-well heterostructure (QWH) devices is that of the material stability when exposed to normal environmental conditions. This is especially true for double-heterostructure and QWH lasers, where cleaved facets are generally used to define the optical cavities and high-composition  $\text{Al}_x\text{Ga}_{1-x}\text{As}$  confining layers are often used to provide optical and charge confinement.<sup>1</sup> Because of the extreme reactivity of Al and its tendency to form various oxygen-rich compounds [ $\text{Al}_2\text{O}_3$ ,  $\text{Al}_2\text{O}_3\cdot\text{H}_2\text{O}$ ,  $\text{Al}_2\text{O}_3\cdot 3\text{H}_2\text{O}$ ,  $\text{AlAsO}_4\cdot 8\text{H}_2\text{O}$ ,  $\text{AlO}(\text{OH})$ ,  $\text{Al}(\text{OH})_3$ ],  $\text{Al}_x\text{Ga}_{1-x}\text{As}$  layers are expected to become more unstable with increasing Al content. This is confirmed by early work on  $\text{Al}_x\text{Ga}_{1-x}\text{As}$ -GaAs solar cells where AlAs layers used as low absorption windows decomposed over time when exposed to room air.<sup>2,3</sup> More recently thick ( $> 0.4\ \mu\text{m}$ ) AlAs buried layers in  $\text{Al}_x\text{Ga}_{1-x}\text{As}$ -AlAs-GaAs QWHs have been found to cause decomposition of the QWH material.<sup>4</sup>

In the present work a more complete account is given of the degradation that occurs in  $\text{Al}_x\text{Ga}_{1-x}\text{As}$ -GaAs QWHs with high-composition ( $x \geq 0.85$ )  $\text{Al}_x\text{Ga}_{1-x}\text{As}$  confining layers. Optical microscopy is used first to identify QWH crystals that have, as described by a colleague,<sup>5</sup> "rusted" (deteriorated and discolored because of hydrolyzation). Then, scanning electron microscopy is used to examine the crystal surfaces and cleaved edges of representative samples. This shows the extent of the degradation, and reveals the layers that are involved in the deterioration process. Next, transmission electron microscopy (TEM) is employed to study the interface between the region of hydrolyzed and intact crystal. Finally, electron dispersion x-ray spectroscopy (EDS) is used to probe these regions to give insight into the deterioration mechanism.

## II. DEGRADATION OF $\text{Al}_x\text{Ga}_{1-x}\text{As}$ QWH MATERIAL

### A. Experimental procedure

The crystals studied in the present work have been grown by metalorganic chemical vapor deposition (MOCVD) on (100) *n*-type GaAs substrates. The first sample of interest dates back to 1978. As usual, for the QWH crystal growth the various sources are trimethylgallium (TMGa), trimethylaluminum (TMA1), and arsine ( $\text{AsH}_3$ ).<sup>6</sup> Typically the crystal growth begins with a GaAs buffer layer  $\sim 1.0\ \mu\text{m}$  thick. Next, a  $\sim 1.0\text{-}\mu\text{m}$ -thick  $\text{Al}_x\text{Ga}_{1-x}\text{As}$  ( $x \geq 0.9$ ) lower confining layer is grown. The active region of one of the QWHs of interest here consists of four GaAs wells ( $L_z \sim 50\ \text{\AA}$ ) separated by three  $\text{Al}_x\text{Ga}_{1-x}\text{As}$  ( $x \geq 0.5$ ) barriers ( $L_B \geq 50\ \text{\AA}$ ). The wafer is capped by a  $\sim 3000\text{-}\text{\AA}$ -thick  $\text{Al}_x\text{Ga}_{1-x}\text{As}$  ( $x \geq 0.9$ ) layer. All of the layers are undoped. For this particular sample the exact composition of the Al-containing layers is not known because of a minor difficulty (at the time of the crystal growth, 1978) with the calibration of the Al mass-flow controller. At the time of the QWH growth x-ray diffraction measurements were not performed to determine exact Al compositions. Despite this difficulty, the sample was found (1978) to be of excellent quality as determined by its capability to operate as a photopumped continuous 300-K laser (e.g., see Ref. 7).

The second crystal of concern here dates back to 1982. The sources for the Al, Ga, and As are once again TMA1, TMGa, and  $\text{AsH}_3$ . The donor and acceptor dopants, Se, Si, and Zn, are provided by  $\text{H}_2\text{Se}$ ,  $\text{SiH}_4$ , and diethylzinc (DEZn). The crystal growth begins with a thick *n*-type GaAs buffer layer and then an  $\text{Al}_{0.75}\text{Ga}_{0.25}\text{As}$  layer ( $\sim 0.75\ \mu\text{m}$ ). This is followed by a thick ( $\sim 0.4\ \mu\text{m}$ ) AlAs lower-confining layer and then the symmetrical active region of the QWH, which consists of a  $\sim 150\text{-}\text{\AA}$  GaAs quantum well

# Hydrolyzation oxidation of $\text{Al}_x\text{Ga}_{1-x}\text{As-AlAs-GaAs}$ quantum well heterostructures and superlattices

J. M. Dallesasse, N. Holonyak, Jr., A. R. Sugg, T. A. Richard,  
and N. El-Zein

*Electrical Engineering Research Laboratory, Center for Compound Semiconductor Microelectronics, and  
Materials Research Laboratory, University of Illinois at Urbana-Champaign, Urbana, Illinois 61801*

(Received 3 October 1990; accepted for publication 23 October 1990)

Data are presented on the conversion (selective conversion) of high-composition  $(\text{AlAs})_x(\text{GaAs})_{1-x}$  layers, e.g., in  $\text{Al}_x\text{Ga}_{1-x}\text{As-AlAs-GaAs}$  quantum well heterostructures and superlattices (SLs), into dense transparent native oxide by reaction with  $\text{H}_2\text{O}$  vapor ( $\text{N}_2$  carrier gas) at elevated temperatures ( $400^\circ\text{C}$ ). Hydrolyzation oxidation of a fine-scale  $\text{AlAs}(L_B)\text{-GaAs}(L_z)$  SL ( $L_B + L_z \lesssim 100 \text{ \AA}$ ), or random alloy  $\text{Al}_x\text{Ga}_{1-x}\text{As}$  ( $x \gtrsim 0.7$ ), is observed to proceed more slowly and uniformly than a coarse-scale "alloy" such as an  $\text{AlAs-GaAs}$  superlattice with  $L_B + L_z \gtrsim 200 \text{ \AA}$ .

Ordinarily the  $\text{Al}_x\text{Ga}_{1-x}\text{As-AlAs-GaAs}$  hetero-system, and its various quantum well heterostructure (QWH) and superlattice (SL) extensions, is viewed as stable against atmospheric deterioration, e.g., hydrolyzation. Recently we have shown that this is not necessarily correct<sup>1,2</sup> and, depending upon  $\text{Al}_x\text{Ga}_{1-x}\text{As}$  composition ( $x \gtrsim 0.7$ ) and layer thickness ( $\gtrsim 0.1 \mu\text{m}$ ), atmospheric hydrolyzation of  $\text{Al}_x\text{Ga}_{1-x}\text{As-AlAs-GaAs}$  QWHs over long time periods (2–10 yr) can be severe. It is, of course, a nuisance to wait, say, ten years, or even one year, to observe this process. For study purposes obviously we wish to accelerate it. A likely way to attempt this is to raise the QWH crystal temperature and pass water vapor over it, the classic method (after Frosch, 1955) to oxidize and mask  $\text{Si}^3$  but thus far not recognized as particularly useful for III-V semiconductors. In this letter we show that instead of destructive hydrolyzation, this procedure results in the formation of smooth dense natural oxides on  $(\text{AlAs})_x(\text{GaAs})_{1-x}$ . A fine scale uniform alloy,  $\text{Al}_x\text{Ga}_{1-x}\text{As}$ , oxidizes more slowly, and a coarser "alloy", for example, as represented by a superlattice (SL), oxidizes "faster" and more completely. In this letter we show that we can render (selectively) a red gap ( $E_g \sim 1.6 \text{ eV}$ )  $\text{AlAs-GaAs}$  SL into yellow-gap (2.1 eV)  $\text{Al}_x\text{Ga}_{1-x}\text{As}$  ( $x \sim 0.8$ ) by impurity-induced layer disordering (IILD),<sup>4</sup> and then change the remaining red-gap SL, where desired, to transparent native oxide by hydrolyzation oxidation.

The experiments we describe here are performed on  $\text{AlAs-GaAs}$  SLs grown by metalorganic chemical vapor deposition as has been described extensively elsewhere.<sup>5</sup> Several ( $\sim 1 \mu\text{m}$  thick) SLs are employed, one (SL1) with  $\text{AlAs}$  barriers of size  $L_B \sim 150 \text{ \AA}$  and  $\text{GaAs}$  wells of width  $L_z \sim 45 \text{ \AA}$  and the second (SL2) with  $L_B(\text{AlAs}) \sim 70 \text{ \AA}$  and  $L_z(\text{GaAs}) \sim 30 \text{ \AA}$ . Although SLs have a special character (size quantization), they can be regarded also as relatively "coarse" (nonstochastic)  $\text{Al}_x\text{Ga}_{1-x}\text{As}$  alloys, with in the present case SL1 roughly two times coarser than SL2. We can render these simply into random (or fine scale) alloys, in a patterned form, by IILD.<sup>4,6</sup> For both SLs of interest here with (100) surfaces this has been done by Zn diffusion from  $\text{ZnAs}_2$  at  $575^\circ\text{C}$  (1/2 h).<sup>4,6</sup> The SLs have been masked with  $\sim 37\text{-}\mu\text{m}$ -diam  $\text{SiO}_2$  disks depos-

ited by chemical vapor deposition and patterned (by standard photolithography) in a rectangular array on  $\sim 76 \mu\text{m}$  centers. After the Zn diffusion and removal of the masking  $\text{SiO}_2$ , as well as the crystal substrates (by the usual mechanical lapping and wet chemical etching), we obtain completely smooth yellow-gap  $\text{Al}_x\text{Ga}_{1-x}\text{As}$  platelets (thickness  $\sim 1 \mu\text{m}$ ) with red-gap SL disks ( $37 \mu\text{m}$  diameter) distributed in a uniform array.<sup>7</sup> We thus have fine scale (yellow) and "coarse" scale (red) alloy in one sample, which can then be oxidized (by "hydrolyzation") at  $400^\circ\text{C}$  in a furnace supplied with a  $\text{N}_2$  carrier gas bubbled through  $\text{H}_2\text{O}$  at a temperature of  $95^\circ\text{C}$ .

Instead of the stained cracked form of destructive atmospheric hydrolyzation shown, for example, by Fig. 1 of Ref. 2, we obtain smooth samples with remarkably shiny surfaces, much shinier than before oxidation. This is the first substantial sign of the formation of a "hard" or useful form of oxide on the samples. A cleaved section of SL1 after heating ( $400^\circ\text{C}$ ) for 3 h is shown in Fig. 1. The top cleaved edge cutting through the  $37\text{-}\mu\text{m}$ -diam SL disks has been arranged to expose the edge of the SL samples (disks) to the heat treatment and oxidation process. The bottom row of disks is exposed to the  $\text{N}_2 + \text{H}_2\text{O}$  vapor only via the surface (front and back). As Fig. 1 shows,  $24 \mu\text{m}$  of each of the upper row of SL disks has converted (edgewise) to oxide, while only some slight delineation or attack is evident on the periphery of the bottom row of disks and, of course, some surface oxide is present. In other words, the upper row of disks is solid and almost totally clear across each disk, while the surrounding IILD  $\text{Al}_x\text{Ga}_{1-x}\text{As}$  ( $x \sim 0.8$ ) remains yellow in appearance and the bottom row of disks red (SL1 with oxide surface).

By reducing the time of the oxidation process to 1 h, we reduce the edge oxide conversion of a SL1 disk to  $\sim 3 \mu\text{m}$  as shown in Fig. 2. A more striking case is shown in Fig. 3 where we have exposed SL2 ( $L_B + L_z \sim 100 \text{ \AA}$ ) to  $400^\circ\text{C}$  heating in a  $\text{N}_2 + \text{H}_2\text{O}$  vapor for 4 h, significantly longer than the case of Fig. 1. Edge oxidation of a SL2 disk penetrates only 2–3  $\mu\text{m}$  in spite of the lengthy oxidation. The surrounding yellow-gap  $\text{Al}_x\text{Ga}_{1-x}\text{As}$  ( $x \sim 0.7$ ) IILD alloy obviously oxidizes also, but not nearly as extensively, in fact, hardly noticeable at all except for the shiny surface.

# Native-oxide stripe-geometry $\text{Al}_x\text{Ga}_{1-x}\text{As}$ -GaAs quantum well heterostructure lasers

J. M. Dallesasse and N. Holonyak, Jr.

*Electrical Engineering Research Laboratory, Center for Compound Semiconductor Microelectronics, and Materials Research Laboratory, University of Illinois at Urbana-Champaign, Urbana, Illinois 61801*

(Received 11 October 1990; accepted for publication 16 November 1990)

Data are presented on the room-temperature continuous (cw) operation of native-oxide single-stripe  $\text{Al}_x\text{Ga}_{1-x}\text{As}$ -GaAs quantum well heterostructure (QWH) lasers. The device quality native oxide is produced by the conversion of high Al composition  $\text{Al}_x\text{Ga}_{1-x}\text{As}$  ( $x \sim 0.8$ ) confining layers via  $\text{H}_2\text{O}$  vapor oxidation ( $400^\circ\text{C}$ ) in a  $\text{N}_2$  carrier gas. The  $10\text{-}\mu\text{m}$ -wide cw 300 K QWH lasers, which are fabricated by simplified processing, have excellent spectral quality and have been operated to powers in excess of 100 mW per facet.

It has long been known in Si technology that the formation of a high quality native oxide ( $\text{SiO}_2$ ) is possible by exposing the crystal to  $\text{H}_2\text{O}$  vapor (steam) in a carrier gas.<sup>1</sup> In fact, Si integrated circuit technology is due largely to the existence of the high quality  $\text{SiO}_2$  native oxide. One difficulty with GaAs and most other III-V compound semiconductors is that they lack a stable native oxide. This difficulty has been overcome to some degree by using other methods such as sputtering, chemical vapor deposition (CVD), and plasma-assisted chemical vapor deposition to apply non-native oxides (or other dielectrics) onto the crystal surface. Recently we have examined the stability of high composition  $\text{Al}_x\text{Ga}_{1-x}\text{As}$  ( $x \geq 0.7$ ) layers in  $\text{Al}_x\text{Ga}_{1-x}\text{As}$ -GaAs quantum well heterostructures (QWHs) and have studied the slow atmospheric deterioration of the QWH material by hydrolysis.<sup>2,3</sup> To speed the process of  $\text{Al}_x\text{Ga}_{1-x}\text{As}$  ( $x \geq 0.7$ ) hydrolysis we have resorted to heating of the QWH crystal in  $\text{H}_2\text{O}$  vapor ( $\text{N}_2$  carrier gas) and have discovered that native oxides of sufficient quality for device use can be formed on the  $\text{Al}_x\text{Ga}_{1-x}\text{As}$  crystal.<sup>4</sup> In fact, AlAs-GaAs superlattices, a "coarser" form of  $(\text{AlAs})_x(\text{GaAs})_{1-x}$  alloy, can be transformed completely to transparent oxide.<sup>4</sup> In this letter the use of this native oxide in the fabrication of gain-guided oxide-stripe QWH lasers is demonstrated. These devices, which are formed by simplified processing, are found to have outstanding performance characteristics.

The epitaxial layers for these laser structures are grown on  $n$ -type (100) GaAs substrates by metalorganic chemical vapor deposition (MOCVD) as described extensively elsewhere.<sup>5</sup> An  $\text{Al}_{0.8}\text{Ga}_{0.2}\text{As}$  lower confining layer is grown after first a GaAs buffer layer. The active region of the QWH is grown next and consists of symmetrical  $\sim 1000 \text{ \AA}$   $\text{Al}_{0.25}\text{Ga}_{0.75}\text{As}$  waveguide layers (undoped) on either side of a  $\sim 400 \text{ \AA}$  GaAs QW. Finally at the top of the QWH a  $p$ -type  $\text{Al}_{0.8}\text{Ga}_{0.2}\text{As}$  confining layer is grown  $\sim 9000 \text{ \AA}$  thick. The entire QWH is capped by a heavily doped  $p$ -type GaAs contact layer ( $\sim 800 \text{ \AA}$  thick).

Diodes are constructed by first depositing  $\sim 1000 \text{ \AA}$  of CVD  $\text{SiO}_2$  on the crystal surface. Using standard photolithography and plasma etching, we define  $10\text{-}\mu\text{m}$ -wide  $\text{SiO}_2$  stripes on the wafer surface for masking purposes. The crystal is then etched in  $\text{H}_2\text{SO}_4\text{:H}_2\text{O}_2\text{:H}_2\text{O}$  (1:8:80) to remove the GaAs contact layer in areas not protected by the

$\text{SiO}_2$  masking stripes. Except in the  $10\text{-}\mu\text{m}$ -wide stripe regions, this exposes the high composition ( $x \sim 0.8$ )  $\text{Al}_x\text{Ga}_{1-x}\text{As}$  upper confining layer. A native oxide is formed from  $\sim 1500 \text{ \AA}$  of the exposed  $\text{Al}_x\text{Ga}_{1-x}\text{As}$  ( $x \sim 0.8$ ) layer by heating the QWH crystal at  $\sim 400^\circ\text{C}$  for 3 h in a  $\text{H}_2\text{O}$  vapor atmosphere produced by passing a  $\text{N}_2$  carrier gas ( $\sim 1.4 \text{ scfh}$ ) through a  $\text{H}_2\text{O}$  bubbler maintained at  $\sim 95^\circ\text{C}$ . The oxide that is produced has a thickness of  $1000\text{--}1500 \text{ \AA}$  and a uniform blue color. Following oxidation of the  $\text{Al}_x\text{Ga}_{1-x}\text{As}$ , the  $\text{SiO}_2$  masking layer is removed by plasma etching ( $\text{CF}_4 + 4\% \text{ O}_2$ ). The native oxide is unaffected by plasma removal of the  $\text{SiO}_2$  layer, which is employed merely to help in processing.

Figure 1 shows a cross section of the crystal before removal of the  $\text{SiO}_2$  masking layer. The vertical arrows in Fig. 1(a) indicate as labeled the thickness of the  $\text{SiO}_2$  layer (left side) and the native oxide layer (to the right). Figure 1(b) shows a cross section in which the native oxide (right side) has been removed by etching in a  $\text{KOH-K}_3\text{Fe}(\text{CN})_6$  mixture. The pair of vertical arrows [Fig. 1(b)] indicates the location of the oxide prior to removal. An important property of the oxidation process is the possibility that it is sensitive to crystal orientation. For example, where the oxide undercuts the  $\text{SiO}_2$  masking stripe and the GaAs contact layer, a tendency exists to develop a crystallographic step on the  $\text{Al}_x\text{Ga}_{1-x}\text{As}$  ( $x \sim 0.8$ ) confining layer. This is shown by the small slanted arrow in Fig. 1(b).

After the  $\text{SiO}_2$  masking stripes are removed, the crystal is sealed in an ampoule for shallow Zn diffusion ( $\text{ZnAs}_2$  source,  $540^\circ\text{C}$ , 25 min) to increase the GaAs stripe contact doping. Then the crystal is metallized (Ti-Pt-Au) across the native oxide onto the exposed GaAs contact stripe. We note that the metallization adheres onto the native oxide much better than on the usual deposited dielectrics, on which frequently the metallization peels. After the  $p$ -type side metallization the crystal is thinned ( $100 \mu\text{m}$ ) from the substrate side and is metallized on the  $n$ -type side (Ge-Au-Ni-Au). The wafer is cleaved into Fabry-Perot bars, and saw-cut stripe-contact sections are attached to Cu heat sinks with In for continuous (cw) 300 K laser operation. Similar saw-cut sections with no contact stripe regions are prepared to check the blocking behavior of the oxide. Figure 2(a) shows the  $I$ - $V$  characteristic of a diode prepared on the QWH crystal in the GaAs contact stripe region, and

# Native-oxide-defined coupled-stripe $\text{Al}_x\text{Ga}_{1-x}\text{As}$ -GaAs quantum well heterostructure lasers

J. M. Dallesasse, N. Holonyak, Jr., D. C. Hall, N. El-Zein, and A. R. Sugg  
*Electrical Engineering Research Laboratory, Center for Compound Semiconductor Microelectronics, and  
 Materials Research Laboratory, University of Illinois at Urbana-Champaign, Urbana, Illinois 61801*

S. C. Smith and R. D. Burnham  
*Amoco Technology Center, Amoco Research Center, Naperville, Illinois 60566*

(Received 26 October 1990; accepted for publication 26 November 1990)

Data are presented on the continuous-wave (cw) room-temperature (300 K) operation of multiple stripe  $\text{Al}_x\text{Ga}_{1-x}\text{As}$ -GaAs quantum well heterostructure (QWH) laser arrays defined with native oxide contact masking. Use of the native  $\text{Al}_x\text{Ga}_{1-x}\text{As}$  ( $x \geq 0.7$ ) oxide allows the fabrication of high-performance devices without depositing foreign oxide or dielectric layers ( $\text{SiO}_2$  or  $\text{Si}_3\text{N}_4$ ). Arrays of ten 5- $\mu\text{m}$ -wide emitters on 7  $\mu\text{m}$  centers are coupled and operate at powers as high as 300 mW per facet, or at wider stripe spacing (5  $\mu\text{m}$  emitters on 10  $\mu\text{m}$  centers) as high as 400 mW per facet. These data indicate that current blocking layers of native oxide, formed from  $\text{Al}_x\text{Ga}_{1-x}\text{As}$  with  $\text{H}_2\text{O}$  vapor in  $\text{N}_2$  carrier gas (400 °C, 3 h), can be used in the construction of high-power multiple stripe QWH arrays with excellent performance characteristics.

We have shown recently that instead of the usual destructive atmospheric hydrolyzation of higher composition  $(\text{AlAs})_x(\text{GaAs})_{1-x}$  ( $x \geq 0.7$ ),<sup>1,2</sup> the alloy can be converted to native oxide by higher temperature heating ( $\geq 400$  °C) in  $\text{H}_2\text{O}$  vapor ( $\text{N}_2$  carrier gas).<sup>3</sup> This has been demonstrated on fine scale (random) alloy and simultaneously, for comparison, on coarse scale alloy as represented by a superlattice ( $x \geq 0.7$ ).<sup>3</sup> Moreover, the native oxide is of sufficient quality so as to be useful in device fabrication,<sup>4</sup> which is of special interest in the present work. One of the more notable features of the native  $\text{Al}_x\text{Ga}_{1-x}\text{As}$  ( $x \geq 0.7$ ) oxide is how well it can be metallized, and thus can be employed in device heat sinking. Also, via ordinary photolithographic processes, the natural oxide permits delineation of device geometries without the need to deposit foreign and thus potentially mismatched dielectric materials (e.g.,  $\text{SiO}_2$  or  $\text{Si}_3\text{N}_4$ ). We show in the present work these features of the natural  $\text{Al}_x\text{Ga}_{1-x}\text{As}$  ( $x \geq 0.7$ ) oxide by constructing, with simplified processing, high-performance ten-stripe  $\text{Al}_x\text{Ga}_{1-x}\text{As}$ -GaAs quantum well heterostructure (QWH) lasers. We show directly the considerable difference in the oxidation behavior of  $\text{Al}_x\text{Ga}_{1-x}\text{As}$  ( $x \geq 0.7$ ) as compared to GaAs, which, relative to oxide formation, is much weaker and readily permits current-contact metallization.

The epitaxial layers for these coupled-stripe QWH lasers are grown on  $n$ -type (100)GaAs substrates by metalorganic chemical vapor deposition (MOCVD) as described extensively elsewhere.<sup>5</sup> A GaAs buffer layer is grown first, followed by an  $n$ -type  $\text{Al}_{0.8}\text{Ga}_{0.2}\text{As}$  lower confining layer. The active region of the QWH is grown next and consists of a  $\sim 400$  Å GaAs QW with  $\sim 1000$  Å  $\text{Al}_{0.25}\text{Ga}_{0.75}\text{As}$  waveguide layers (undoped) on either side. Finally, a  $p$ -type  $\text{Al}_{0.8}\text{Ga}_{0.2}\text{As}$  confining layer ( $\sim 9000$  Å) is grown on top of the active region. The entire QWH is capped by a heavily doped  $p$ -type GaAs contact layer ( $\sim 800$  Å thick).

The GaAs contact layer is removed where desired to provide access to the upper confining layer for formation of the native oxide.<sup>3</sup> As we show here, the GaAs layer does not oxidize readily, and consequently can be used directly as a mask (and then contact layer) in forming the native oxide on the upper confining layer. Standard photolithography is used to mask sets of ten 5- $\mu\text{m}$ -wide GaAs stripes that are located 2  $\mu\text{m}$  apart (7  $\mu\text{m}$  center-to-center spacing). The GaAs between the stripes (2  $\mu\text{m}$  width), as well as the GaAs between sets of stripes, is removed with  $\text{H}_2\text{SO}_4\text{:H}_2\text{O}_2\text{:H}_2\text{O}$  (1:8:80). This exposes the high composition  $\text{Al}_x\text{Ga}_{1-x}\text{As}$  ( $x \sim 0.8$ ) upper confining layer for oxidation after removal of the photoresist. The  $\text{Al}_x\text{Ga}_{1-x}\text{As}$  oxidation is accomplished by heating the QWH at 400 °C (3 h) in a  $\text{H}_2\text{O}$  vapor atmosphere obtained by passing  $\text{N}_2$  carrier gas ( $\sim 1.4$  scfh) through a  $\text{H}_2\text{O}$  bubbler maintained at 95 °C.<sup>3,4</sup>

The QWH crystal after oxidation is shown in Fig. 1(a). The 5  $\mu\text{m}$  GaAs contact stripes remain shiny (silvery) and basically unaffected by the oxidation. The rest of the crystal, including the 2  $\mu\text{m}$  regions between the GaAs stripes, is covered with a uniform oxide that appears blue in color and, as is shown elsewhere,<sup>4</sup> is 1000–1500 Å thick. Besides the significant difference in contacting behavior (conducting versus insulating), this is direct evidence [Fig. 1(a)] of the different oxidation behavior of  $\text{Al}_x\text{Ga}_{1-x}\text{As}$  at one extreme  $x = 0$  (GaAs) and at the other,  $x \sim 1$  (AlAs).

After the QWH is metallized (Ti-Pt-Au) across its entire surface it appears as shown in Fig. 1(b). Before metallization the crystal is Zn diffused ( $\text{ZnAs}_2$ , 540 °C, 25 min) to a shallow depth to improve the contact on the GaAs stripes. This procedure obviously does not require any special masking. The crystal is thinned to  $\sim 100$   $\mu\text{m}$  and is metallized on the substrate side (Ge-Au-Ni-Au), and is cleaved into Fabry-Perot resonator strips that are then saw-cut into separate ten-stripe dies. These are attached to Cu with In on the stripe side for heat sinking and

# Native-oxide masked impurity-induced layer disordering of $\text{Al}_x\text{Ga}_{1-x}\text{As}$ quantum well heterostructures

J. M. Dallesasse,<sup>a)</sup> N. Holonyak, Jr., N. El-Zein, T. A. Richard, F. A. Kish, and A. R. Sugg  
Electrical Engineering Research Laboratory, Center for Compound Semiconductor Microelectronics,  
and Materials Research Laboratory, University of Illinois at Urbana-Champaign, Urbana, Illinois 61801

R. D. Burnham and S. C. Smith

Amoco Technology Company, Amoco Research Center, Naperville, Illinois 60566

(Received 21 November 1990; accepted for publication 4 January 1991)

Data are presented showing that the native oxide that can be formed on high Al composition  $\text{Al}_x\text{Ga}_{1-x}\text{As}$  ( $x \geq 0.7$ ) confining layers on  $\text{Al}_y\text{Ga}_{1-y}\text{As-Al}_z\text{Ga}_{1-z}\text{As}$  ( $y > z$ ) superlattices or quantum well heterostructures serves as an effective mask against impurity diffusion (Zn or Si), and thus against impurity-induced layer disordering. The high quality native oxide is produced by the conversion of high Al composition  $\text{Al}_x\text{Ga}_{1-x}\text{As}$  ( $x \geq 0.7$ ) confining layers, which can be grown on a variety of heterostructures, via  $\text{H}_2\text{O}$  vapor oxidation ( $\geq 400^\circ\text{C}$ ) in an  $\text{N}_2$  carrier gas.

Ordinarily high Al composition  $\text{Al}_x\text{Ga}_{1-x}\text{As}$  ( $x \geq 0.7$ ) is susceptible to destructive (atmospheric) hydrolyzation<sup>1,2</sup> but not if heated at high enough temperature ( $\geq 400^\circ\text{C}$ ) in a rich  $\text{H}_2\text{O}$ -vapor ambient.<sup>3</sup> At higher temperatures and high  $\text{H}_2\text{O}$  vapor pressure, more stable phases of the oxide form,<sup>3,4</sup> which indeed are useful in device applications.<sup>5,6</sup> For even greater usefulness an important question is that of the masking capability of the natural oxide that can be formed on  $\text{Al}_x\text{Ga}_{1-x}\text{As}$  ( $x > 0.7$ ). In this letter we demonstrate this behavior via Zn diffusion and impurity-induced layer disordering (IILD),<sup>7-10</sup> i.e., layer disordering of a bare  $\text{Al}_x\text{Ga}_{1-x}\text{As-GaAs}$  superlattice (SL) or quantum well heterostructure (QWH) crystal in contrast to masking of the SL or QWH by the natural oxide. In the latter case (oxide masking) the quantum well (QW) and superlattice (SL) layers are preserved.

The SL and QWH crystals used in these experiments are grown on (100)GaAs substrates by metalorganic chemical vapor deposition (MOCVD) as described extensively elsewhere.<sup>11</sup> In the case of the SL crystal (crystal No. 1), a GaAs buffer layer is grown first and next an undoped  $\text{Al}_{0.8}\text{Ga}_{0.2}\text{As}$  lower confining layer ( $\sim 0.1 \mu\text{m}$ ). Then the SL consisting of 40 GaAs wells ( $L_z \sim 110 \text{ \AA}$ ) and 41  $\text{Al}_{0.4}\text{Ga}_{0.6}\text{As}$  barriers ( $L_B \sim 150 \text{ \AA}$ ) is grown. The total SL thickness is  $\sim 1.05 \mu\text{m}$  (see Fig. 1). Finally a  $1000 \text{ \AA}$   $\text{Al}_{0.8}\text{Ga}_{0.2}\text{As}$  confining layer is grown on top of the SL. The structure is capped with a  $3000 \text{ \AA}$  GaAs layer. The first part of the MOCVD QWH (crystal No. 2) is an  $n$ -type GaAs buffer layer ( $\sim 0.5 \mu\text{m}$ ), which is followed by an  $n$ -type  $\text{Al}_{0.25}\text{Ga}_{0.75}\text{As}$  intermediate layer. An  $n$ -type  $\text{Al}_{0.8}\text{Ga}_{0.2}\text{As}$  lower confining layer is grown next. This is followed by the QWH active region, which is a  $\sim 200 \text{ \AA}$   $\text{Al}_{0.06}\text{Ga}_{0.94}\text{As}$  QW sandwiched by two undoped  $\sim 1000 \text{ \AA}$   $\text{Al}_{0.25}\text{Ga}_{0.75}\text{As}$  waveguide (WG) layers. Finally a  $p$ -type  $\text{Al}_{0.8}\text{Ga}_{0.2}\text{As}$  confining layer ( $\sim 9000 \text{ \AA}$ ) is grown on top of the active region. The entire QWH, which is useful in laser diode construction, is capped by a heavily doped

$p$ -type GaAs contact layer ( $\sim 800 \text{ \AA}$ ).

The GaAs cap layer on either the SL or the QWH is removed to allow the upper AlGaAs confining layer ( $x \sim 0.8$ ) to be oxidized.<sup>3</sup> The presence of Ga in the oxidized layer and at the oxide-semiconductor interface does not adversely affect the structure of the oxide since the Ga-O and Al-O compounds form structural isomorphs, and  $\text{Al}_2\text{O}_3$  and  $\text{Ga}_2\text{O}_3$  form a solid solution over the entire compositional range.<sup>4</sup> The  $\text{Al}_x\text{Ga}_{1-x}\text{As}$  oxidation is accomplished by heating the samples at  $400^\circ\text{C}$  (3 h) in an  $\text{H}_2\text{O}$  vapor atmosphere obtained by passing  $\text{N}_2$  carrier gas ( $\sim 1.5 \text{ scfh}$ ) through an  $\text{H}_2\text{O}$  bubbler maintained at  $95^\circ\text{C}$ .<sup>3,4</sup> Lower temperatures are not used so as not to form poorer oxides.<sup>4</sup>

In order to effect selective Zn diffusion and layer disordering of the SL sample (crystal No. 1),<sup>7-10</sup> a photoresist stripe pattern ( $20 \mu\text{m}$  stripes on  $50 \mu\text{m}$  centers) is defined on top of the oxide. Using a  $\text{NH}_4\text{F}:\text{HF}$  (7:1) buffered HF

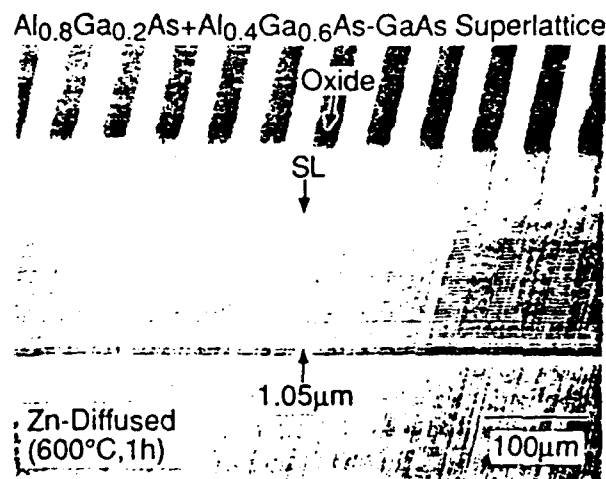


FIG. 1. Shallow-angle beveled cross section of a  $1.05 \mu\text{m}$   $\text{Al}_{0.8}\text{Ga}_{0.2}\text{As-Al}_{0.4}\text{Ga}_{0.6}\text{As-GaAs}$  SL ( $L_z \sim 110 \text{ \AA}$ ,  $L_B \sim 150 \text{ \AA}$ ) following Zn diffusion with  $20 \mu\text{m}$  natural-oxide masking stripes (top) on the crystal surface. The lower part of the slant cross section shows regions where the superlattice is disordered (regions not masked by the oxide) alternating with regions where the superlattice is intact (regions masked by the oxide)

<sup>a)</sup>Now at Amoco Technology Company, Amoco Research Center, Naperville, IL 60566.

## Native oxide stabilization of AlAs-GaAs heterostructures

A. R. Sugg, N. Holonyak, Jr., J. E. Baker, F. A. Kish,<sup>a)</sup> and J. M. Dallesasse<sup>b)</sup>  
*Electrical Engineering Research Laboratory, Center for Compound Semiconductor Microelectronics,  
 and Materials Research Laboratory, University of Illinois at Urbana-Champaign, Urbana, Illinois 61801*

(Received 18 December 1990; accepted for publication 14 January 1991)

Data are presented on the stabilization of AlAs-GaAs heterostructures against atmospheric (destructive) hydrolysis using the native oxide that can be formed ( $N_2 + H_2O$ , 400 °C, 3 h) on the AlAs layer. The  $\sim 0.1\text{-}\mu\text{m}$ -thick native oxide formed from the AlAs layer is shown to be stable with aging ( $\sim 100$  days), while unoxidized samples degrade through the AlAs ( $0.1\text{ }\mu\text{m}$ ) down into the GaAs as deep as  $\sim 1\text{ }\mu\text{m}$ . Relative to oxides formed ( $\sim 25\text{ }^\circ\text{C}$ ) on AlAs (or  $Al_xGa_{1-x}As$ ,  $x \geq 0.7$ ) under atmospheric conditions (hydrolysis), oxides formed (via  $N_2 + H_2O$ ) at higher temperatures ( $\geq 400\text{ }^\circ\text{C}$ ) are much more stable and seal the underlying crystal (e.g., GaAs).

The environmental degradation (hydrolysis) of high Al composition  $Al_xGa_{1-x}As$  ( $x \geq 0.7$ ) in AlGaAs-GaAs quantum well heterostructures (QWHs) can be the basis for serious reliability problems.<sup>1,2</sup> Recently device-quality native oxide formed on QWHs from  $Al_xGa_{1-x}As$  ( $x \geq 0.8$ ) via an elevated-temperature ( $\geq 400\text{ }^\circ\text{C}$ ) water vapor process has been demonstrated<sup>3,4</sup> and changes the nature of this problem. In a rich water vapor ambient at higher temperatures ( $\geq 400\text{ }^\circ\text{C}$ ) more stable oxides form than those created in atmospheric conditions at room temperature.<sup>5</sup> In this letter we demonstrate the stabilizing nature of this native oxide on AlAs-GaAs heterostructures, which is in sharp contrast to the destructive hydrolyzation of atmospheric processes. An AlAs-GaAs heterostructure is oxidized and compared to the same structure that is allowed to hydrolyze naturally. The oxidized crystal, once sealed, is unaffected by the destructive character of atmospheric hydrolysis. In contrast, atmospheric hydrolysis (80–100 days) of AlAs-GaAs is shown to affect the AlAs layer ( $\sim 0.1\text{ }\mu\text{m}$ ) itself, as well as  $\sim 1\text{ }\mu\text{m}$  of the underlying GaAs.

The crystals used in this experiment are grown by metalorganic chemical vapor deposition (MOCVD) on {100}  $n$ -type GaAs substrates<sup>6</sup> in an EMCORE GS 3000 DFM reactor at 760 °C. The crystal growth pressure, V/III ratio, and growth rate are 100 Torr, 60, and  $\sim 1000\text{ }\text{\AA}/\text{min}$ , respectively. An undoped  $\sim 0.5\text{ }\mu\text{m}$  GaAs layer is grown first, followed by a  $\sim 0.1\text{-}\mu\text{m}$ -thick nominally undoped AlAs layer. The crystal is then cleaved in two, half of which is then exposed to atmospheric conditions at room temperature. The other half is oxidized at 400 °C (3 h) in an  $H_2O$  vapor atmosphere obtained by passing  $N_2$  carrier gas ( $\sim 1.5\text{ scfh}$ ) through an  $H_2O$  bubbler maintained at 95 °C.<sup>3,4</sup>

The two types of samples, (a) and (b), are then exposed to identical atmospheric conditions. Within hours unoxidized crystals begin to degrade in color to a yellowish brown, while oxidized wafers maintain a uniform blue appearance. Figure 1 shows (Nomarski image) the surface of

an (a) crystal and that of a (b) crystal after, in both cases, atmospheric exposure for 100 days. Obviously the figure does not show the yellow-brown stained color of the hydrolyzed (a) sample, nor the blue color of the oxidized (b) sample. The surface of (a) is clearly "rougher" than that of (b), which agrees with the even more extreme case of Fig. 1 of Ref. 2. The oxidized surface is smoother than the hydrolyzed surface and the cleaved edge is intact, whereas the edge of the hydrolyzed sample shows sign of destructive attack (roughening).

Figure 2 is a scanning electron microscope (SEM) image of the edges of the (a) and (b) samples of Fig. 1. The sample edges are unstained cleaved cross sections that are aged 100 days. The atmospherically hydrolyzed (a) sample shows  $\sim 1\text{ }\mu\text{m}$  of chemical attack into the crystal (indicated by the vertical arrows), which is well beyond the  $\sim 0.1\text{ }\mu\text{m}$  AlAs top layer of the as-grown crystal. In contrast, the cross section of the oxidized (b) sample exhibits a  $\sim 0.1\text{ }\mu\text{m}$  oxide layer (shown between the vertical arrows), agreeing more or less with the initial AlAs thickness, and with no perceptible degradation. The cross section of the hydrolyzed sample appears to be nonuniformly etched. This is remarkable considering that the sample is not stained to highlight this layer.

The results of secondary-ion mass spectrometer (SIMS) analysis on (a) and (b) samples after 80 days are

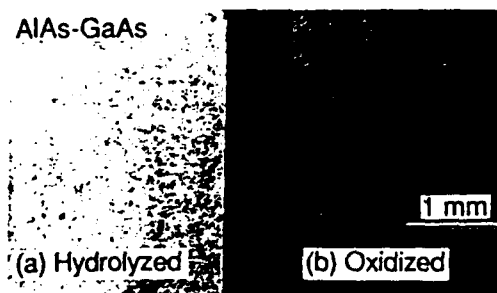


FIG. 1. Photograph (Nomarski image) after 100 days of (a) an atmospherically hydrolyzed and (b) an oxidized ( $N_2 + H_2O$ , 400 °C, 3 h) AlAs-GaAs heterostructure. The unoxidized sample (a) shows the characteristic roughening of atmospheric hydrolysis, while the oxidized sample (b), which is covered with a smooth "blue" oxide, is unaffected by the aging process.

<sup>a)</sup>AT&T Doctoral Fellow.

<sup>b)</sup>Now at Amoco Technology Company, Amoco Research Center, Naperville, IL 60566.

# Low-threshold disorder-defined native-oxide delineated buried-heterostructure $\text{Al}_x\text{Ga}_{1-x}\text{As}$ -GaAs quantum well lasers

F. A. Kish,<sup>a)</sup> S. J. Caracci, N. Holonyak, Jr., J. M. Dallesasse,<sup>b)</sup> and G. E. Höfler

*Electrical Engineering Research Laboratory, Center for Compound Semiconductor Microelectronics, and Materials Research Laboratory, University of Illinois at Urbana-Champaign, Urbana, Illinois 61801*

R. D. Burnham and S. C. Smith

*Amoco Technology Company, Amoco Research Center, Naperville, Illinois 60566*

(Received 3 December 1990; accepted for publication 13 February 1991)

Impurity-induced layer disordering (IILD) along with oxidation (native oxide) of high-gap  $\text{Al}_x\text{Ga}_{1-x}\text{As}$  confining layers is employed to fabricate low-threshold stripe-geometry buried-heterostructure  $\text{Al}_x\text{Ga}_{1-x}\text{As}$ -GaAs quantum well heterostructure (QWH) lasers. Silicon IILD is used to intermix the quantum well and waveguide regions with the surrounding confining layers (beyond the laser stripe) to provide optical and current confinement in the QW region of the stripe. The high-gap  $\text{Al}_x\text{Ga}_{1-x}\text{As}$  upper confining layer is oxidized in a self-aligned configuration defined by the contact stripe and reduces IILD leakage currents at the crystal surface and diffused shunt junctions.  $\text{Al}_x\text{Ga}_{1-x}\text{As}$ -GaAs QWH lasers fabricated by this method have continuous 300 K threshold currents as low as 5 mA and powers > 31 mW/facet for  $\sim 3\text{-}\mu\text{m}$ -wide active regions.

By means of relatively simple processing, impurity-induced layer disordering (IILD)<sup>1,2</sup> has been employed to produce very high performance planar buried-heterostructure (BH) quantum well heterostructure (QWH) lasers.<sup>3</sup> Various dopants and diffusion techniques have been employed to fabricate disorder-defined BH lasers, including (1) Si solid-source diffusion,<sup>4</sup> (2) Si implantation and annealing,<sup>5</sup> (3) Ge diffusion from the vapor,<sup>6</sup> (4) Zn diffusion from the vapor,<sup>7</sup> (5) Si-O diffusion from Al-reduced  $\text{SiO}_2$ ,<sup>8</sup> (6) Si diffusion from Al-reduced  $\text{Si/Si}_3\text{N}_4$  via rapid thermal annealing,<sup>9</sup> and (7) Si diffusion from laser-melted  $\text{Si}_3\text{N}_4$ .<sup>10</sup> Many of these have the disadvantage that they form a very highly conducting layer at the crystal surface. This conducting layer is a source of leakage, and thus increases laser threshold currents. Under some conditions the alloying is so severe that a relatively deep proton implant is required to passivate the leakage regions to insure low-threshold laser operation.<sup>9,11</sup> In this letter a self-aligned process is reported in which these surfaces are converted to current blocking native oxide. The oxide passivates the surface, reducing surface and shunt junction leakage currents, and thus yielding an improved form of low-threshold disorder-defined BH  $\text{Al}_x\text{Ga}_{1-x}\text{As}$ -GaAs quantum well heterostructure laser.

The QWH laser crystal employed in this work is grown by metalorganic chemical vapor deposition (MOCVD)<sup>12</sup> on an  $n$ -type substrate. The growth begins with  $n$ -type buffer layers of GaAs ( $\sim 0.5\text{ }\mu\text{m}$ ) and  $\text{Al}_{0.25}\text{Ga}_{0.75}\text{As}$  ( $\sim 1\text{ }\mu\text{m}$ ). This is followed by the growth of a  $\sim 1.1\text{ }\mu\text{m}$   $\text{Al}_{0.77}\text{Ga}_{0.23}\text{As}$   $n$ -type lower confining layer, a  $\sim 2000\text{ }\text{\AA}$   $\text{Al}_{0.25}\text{Ga}_{0.75}\text{As}$  undoped waveguide region, a  $\sim 1.1\text{ }\mu\text{m}$   $\text{Al}_{0.8}\text{Ga}_{0.2}\text{As}$   $p$ -type upper confining layer, and a  $\sim 0.1\text{ }\mu\text{m}$

$p$ -type GaAs cap. In the center of the waveguide is a  $\sim 200\text{ }\text{\AA}$   $\text{Al}_{0.06}\text{Ga}_{0.94}\text{As}$  quantum well (undoped).

The laser diode fabrication process begins with a shallow Zn diffusion over the entire surface in an evacuated quartz ampoule (540 °C, 30 min). The shallow  $p^+$  layer formed by the diffusion helps control lateral Si diffusion at the crystal surface under the masked regions in later processing steps.<sup>6</sup> After Zn diffusion, the crystal is encapsulated with  $\sim 1000\text{ }\text{\AA}$  of  $\text{Si}_3\text{N}_4$  deposited by chemical vapor deposition (CVD) at 720 °C. The  $\text{Si}_3\text{N}_4$  is patterned with photoresist and etched with a  $\text{CF}_4$  plasma into two choices of stripe width, 4 and 6  $\mu\text{m}$ . The photoresist is removed, and the remaining  $\text{Si}_3\text{N}_4$  stripes serve as masks for chemical etching ( $\text{H}_2\text{SO}_4\text{:H}_2\text{O}_2\text{:H}_2\text{O}$ , 1:8:80) of the GaAs contact layer, thus leaving the high-gap  $\text{Al}_{0.8}\text{Ga}_{0.2}\text{As}$  upper confining layer exposed. Following stripe delineation, CVD is used to deposit a  $\sim 300\text{ }\text{\AA}$  Si layer (550 °C) and a  $\sim 1700\text{ }\text{\AA}$   $\text{SiO}_2$  cap layer (400 °C). The crystal is then sealed in an evacuated quartz ampoule and annealed with excess As at 850 °C for 6.5 h. The high-temperature anneal results in Si diffusion and IILD outside of the GaAs contact stripes. All encapsulants are then removed by etching with a  $\text{CF}_4$  plasma, and the crystal is placed in an open tube furnace (supplied with a  $\text{N}_2$  carrier gas bubbled through  $\text{H}_2\text{O}$  at 95 °C) at 400 °C for 3 h. This process results in oxidation of  $\sim 2000\text{ }\text{\AA}$  of the exposed high-gap upper confining layers at the edge and beyond the GaAs contact stripe regions.<sup>13</sup> No oxide is formed on the GaAs contact stripes due to the selectivity of the oxidation process.<sup>14</sup> Native oxides are only formed in areas of high Al composition, resulting in self-aligned contact stripes. Following the oxidation process, the wafer is sealed in an ampoule with a  $\text{ZnAs}_2$  source, and is annealed at 540 °C for 30 min to form a shallow, heavily doped  $p$ -type region only in the contact area. (We note that the native oxide provides an effective mask for the Zn diffusion.)<sup>15</sup> Samples are

<sup>a)</sup>AT&T Doctoral Fellow.

<sup>b)</sup>Now at Amoco Technology Company, Amoco Research Center, Naperville, Illinois 60566.



# Native-oxide coupled-stripe $\text{Al}_y\text{Ga}_{1-y}\text{As-GaAs-In}_x\text{Ga}_{1-x}\text{As}$ quantum well heterostructure lasers

T. A. Richard, F. A. Kish, N. Holonyak, Jr., J. M. Dallesasse,<sup>a)</sup> K. C. Hsieh, and M. J. Ries

*Electrical Engineering Research Laboratory, Center for Compound Semiconductor Microelectronics, and Materials Research Laboratory, University of Illinois at Urbana-Champaign, Urbana, Illinois 61801*

P. Gavrilovic, K. Meehan, and J. E. Williams

*Microelectronics Laboratory, Polaroid Corporation, Cambridge, Massachusetts 02139*

(Received 7 February 1991; accepted for publication 3 March 1991)

Data are presented on a high-performance native-oxide coupled-stripe  $\text{Al}_y\text{Ga}_{1-y}\text{As-GaAs-In}_x\text{Ga}_{1-x}\text{As}$  quantum well heterostructure laser realized by the recently introduced simple process of "wet" oxidation ( $\text{H}_2\text{O}$  vapor +  $\text{N}_2$ ,  $\geq 400^\circ\text{C}$ , 3 h) of the upper  $\text{Al}_y\text{Ga}_{1-y}\text{As}$  confining layer. If the native oxide between active stripes (ten  $5\text{ }\mu\text{m}$  stripes on  $10\text{ }\mu\text{m}$  centers) is brought into closer proximity with the waveguide and quantum well region (i.e., from  $0.53$  to  $0.4\text{ }\mu\text{m}$ ), the 10-stripe laser operates decoupled because of increased (coupling) absorption losses and some index guiding.

A standard form of semiconductor laser that, among other purposes, is routinely used to evaluate heterostructure crystals is the deposited oxide single- or multiple-stripe device. This form of stripe-geometry laser consists of simply the externally deposited oxide, photolithographically defined and etched stripe openings on the crystal, and contact metallization across the stripe openings and the oxide (followed by crystal cleaving, sawing, and die mounting). Recently we have simplified this structure further by converting, where desired (stripe geometry), the upper  $\text{Al}_y\text{Ga}_{1-y}\text{As}$  ( $y \geq 0.7$ ) confining layers of  $\text{Al}_y\text{Ga}_{1-y}\text{As-GaAs}$  quantum well heterostructures (QWHs) to the natural oxide by the simple process of "wet" oxidation ( $\text{H}_2\text{O}$  vapor +  $\text{N}_2$ ,  $\geq 400^\circ\text{C}$ , 3 h).<sup>1-3</sup> In this letter we demonstrate the conditions for use of this simple procedure to realize relatively high-power coupled-stripe  $\text{Al}_y\text{Ga}_{1-y}\text{As-GaAs-In}_x\text{Ga}_{1-x}\text{As}$  QWH lasers. We show at what distance (thickness) from the QW active region the native oxide between stripes leads to increased (coupling) absorption loss and to some index guiding, and thus loss of stripe-to-stripe coupling.

The quantum well heterostructure (QWH) crystal used in this work is grown on a Si-doped GaAs substrate by metalorganic chemical vapor deposition (MOCVD).<sup>4</sup> The growth temperature is  $800^\circ\text{C}$  except for the  $\text{In}_x\text{Ga}_{1-x}\text{As}$  quantum well (QW), which is grown at  $630^\circ\text{C}$  to prevent In desorption. The growth of the epitaxial layers consists, first, of a GaAs buffer layer, followed by an  $n$ -type (Se)  $\text{Al}_{0.8}\text{Ga}_{0.2}\text{As}$  lower confining layer ( $\sim 1.25\text{ }\mu\text{m}$ ), and then the active region and waveguide layers ( $\sim 3000\text{ }\text{\AA}$ ). The nominally undoped active region and waveguide (WG) consist of an  $\text{Al}_{0.3}\text{Ga}_{0.7}\text{As}$  WG on either side of a GaAs layer ( $\sim 640\text{ }\text{\AA}$ ) with an  $\text{In}_{0.1}\text{Ga}_{0.9}\text{As}$  QW ( $\sim 100\text{ }\text{\AA}$ ) at its center. Finally a  $p$ -type (Mg)  $\text{Al}_{0.8}\text{Ga}_{0.2}\text{As}$  upper confining layer ( $\sim 6000\text{ }\text{\AA}$ ) is grown

with a  $p$ -type (Mg + Zn) GaAs contact layer ( $\sim 1000\text{ }\text{\AA}$ ) on top.

The fabrication of the coupled-stripe laser begins with standard photolithographic techniques to define arrays of ten  $5\text{-}\mu\text{m}$ -wide photoresist stripes with a center-to-center spacing of  $10\text{ }\mu\text{m}$ . These stripes are then used as a mask for an  $\text{H}_2\text{SO}_4\text{:H}_2\text{O}_2\text{:H}_2\text{O}$  (1:8:80) etch to remove (except under the mask) the GaAs cap. The photoresist is removed leaving the exposed  $\text{Al}_{0.8}\text{Ga}_{0.2}\text{As}$  upper confining layer between and outside of the stripes ready for "wet" oxidation.<sup>1-3</sup> The crystal is placed in an  $\text{H}_2\text{O}$  vapor atmosphere at  $400^\circ\text{C}$  for 3 h. The  $\text{H}_2\text{O}$  vapor is supplied by an  $\text{N}_2$  carrier gas ( $\sim 1.4\text{ scfh}$ ) flowing through a heated  $\text{H}_2\text{O}$  bubbler ( $\sim 95^\circ\text{C}$ ).

At this point a scanning electron microscope (SEM) image (Fig. 1) is taken. Figure 1 shows the cross section near the edge of one of the GaAs contact stripes. The oxide, which is recessed (left side), is approximately the same thickness ( $\sim 1000\text{ }\text{\AA}$ ) as the stripe GaAs contact layer. Also shown is the oxide undercutting the GaAs layer without noticeably affecting it.

After the oxidation process, the crystal is sealed in an evacuated quartz ampoule with  $\text{ZnAs}_2$  for a 15 min shallow Zn diffusion at  $540^\circ\text{C}$  to improve contacting. The native oxide itself is used to mask the Zn diffusion between the active stripes.<sup>5</sup> The crystal is then lapped and polished from the substrate side to a thickness of  $\sim 125\text{ }\mu\text{m}$ . The crystal is metallized with Ti-Pt-Au for the  $p$ -type contact and an alloyed Ge-Au-Ni-Au for the  $n$ -type contact. Finally, the crystal is cleaved ( $\sim 375\text{ }\mu\text{m}$  long) and saw-cut into individual dies and mounted on In-coated Cu heat sinks for testing.

Figure 2 shows the cw 300 K operation of a typical device mounted  $p$  side down. The array has a laser threshold (uncoated facets) of 95 mA at a wavelength of  $\sim 913\text{ nm}$ . The spectral output at 150 mA is shown in the inset. The laser arrays have a differential quantum efficiency of 42% and a peak output power of over 350 mW per facet (before burn-out).

<sup>a)</sup>Now at Amoco, Naperville, Illinois 60566.



# Native-oxide stripe-geometry $\text{In}_{0.5}(\text{Al}_x\text{Ga}_{1-x})_{0.5}\text{P}-\text{In}_{0.5}\text{Ga}_{0.5}\text{P}$ heterostructure laser diodes

F. A. Kish,<sup>a)</sup> S. J. Caracci,<sup>b)</sup> N. Holonyak, Jr., J. M. Dallesasse,<sup>c)</sup> and A. R. Sugg  
*Electrical Engineering Research Laboratory, Center for Compound Semiconductor Microelectronics,  
and Materials Research Laboratory, University of Illinois at Urbana-Champaign, Urbana,  
Illinois 61801*

R. M. Fletcher, C. P. Kuo, T. D. Osentowski, and M. G. Craford  
*Hewlett-Packard Company, Optoelectronics Division, San Jose, California 95131*

(Received 26 April 1991; accepted for publication 15 May 1991)

Data are presented demonstrating the formation of stable, device-quality native oxides from high Al composition  $\text{In}_{0.5}(\text{Al}_x\text{Ga}_{1-x})_{0.5}\text{P}$  ( $x \sim 0.9$ ) via reaction with  $\text{H}_2\text{O}$  vapor (in  $\text{N}_2$  carrier gas) at elevated temperatures ( $>500^\circ\text{C}$ ). The oxide exhibits excellent current-blocking characteristics and is employed to fabricate continuous room-temperature stripe-geometry  $\text{In}_{0.5}(\text{Al}_x\text{Ga}_{1-x})_{0.5}\text{P}-\text{In}_{0.5}\text{Ga}_{0.5}\text{P}$  double-heterostructure laser diodes.

The study of the problem of degradation of high composition  $\text{Al}_x\text{Ga}_{1-x}\text{As}$  ( $x > 0.7$ ) on  $\text{Al}_x\text{Ga}_{1-x}\text{As}-\text{Al}_y\text{Ga}_{1-y}\text{As}-\text{GaAs}$  quantum well heterostructures<sup>1,2</sup> has led to the discovery that device-quality native oxides can be formed from high-gap  $\text{Al}_x\text{Ga}_{1-x}\text{As}$  under proper conditions,<sup>3</sup> e.g., at temperatures  $\geq 400^\circ\text{C}$  by reaction with  $\text{H}_2\text{O}$  vapor in a  $\text{N}_2$  carrier gas. The  $\text{Al}_x\text{Ga}_{1-x}\text{As}$  native oxide, with excellent insulating properties,<sup>4</sup> has already proven to be quite useful in such applications as impurity masking,<sup>5</sup> stripe-geometry laser diode fabrication,<sup>4,6</sup> AlAs layer stabilization,<sup>7</sup> reduction of parasitic leakage currents,<sup>8</sup> and formation of optical waveguides.<sup>9</sup> These desirable qualities are attributable to the formation of aluminum oxide and hydroxide compounds during the "wet" oxidation process.<sup>7</sup> These results suggest other III-V semiconductor materials containing an appreciable amount of Al are candidates for conversion to various forms of native oxides. In this letter we extend the "wet" oxidation procedure employed successfully on  $\text{Al}_x\text{Ga}_{1-x}\text{As}$  to other III-V systems. Specifically, we demonstrate formation of stable, device-quality native oxides in the  $\text{In}_{0.5}(\text{Al}_x\text{Ga}_{1-x})_{0.5}\text{P}$  system. The oxide is of sufficient quality to be employed in fabrication of continuous (cw) room-temperature ( $23^\circ\text{C}$ )  $\text{In}_{0.5}(\text{Al}_x\text{Ga}_{1-x})_{0.5}\text{P}-\text{In}_{0.5}\text{Ga}_{0.5}\text{P}$  double-heterostructure (DH) laser diodes.

The crystal employed in this work is grown on an  $n$ -type GaAs substrate by metalorganic chemical vapor deposition (MOCVD) as described extensively elsewhere.<sup>10</sup> The epitaxial layers of interest consist of an  $\sim 0.8\text{ }\mu\text{m}$   $n$ -type  $\text{In}_{0.5}(\text{Al}_{0.9}\text{Ga}_{0.1})_{0.5}\text{P}$  lower confining layer, a  $\sim 1000\text{ }\text{\AA}$   $\text{In}_{0.5}\text{Ga}_{0.5}\text{P}$  active region (undoped), an  $\sim 0.8\text{ }\mu\text{m}$   $p$ -type  $\text{In}_{0.5}(\text{Al}_{0.9}\text{Ga}_{0.1})_{0.5}\text{P}$  upper confining layer, and a low-gap  $p$ -type contact layer.

The device fabrication begins with deposition of  $\sim 1000\text{ }\text{\AA}$  of  $\text{Si}_3\text{N}_4$  by chemical vapor deposition at  $720^\circ\text{C}$  which is then patterned into  $10\text{ }\mu\text{m}$  stripes. The  $\text{Si}_3\text{N}_4$

serves as a mask for the chemical etching of the contact layer using 0.1% Br-methanol, leaving the high-gap  $\text{In}_{0.5}(\text{Al}_{0.9}\text{Ga}_{0.1})_{0.5}\text{P}$  upper confining layer exposed outside of the laser stripe. The  $\text{Si}_3\text{N}_4$  also prevents any subsequent oxidation of the contact layer. The sample is next placed in an open tube furnace (supplied with a  $\text{N}_2$  carrier gas bubbled through  $\text{H}_2\text{O}$  at  $95^\circ\text{C}$ ) at  $500^\circ\text{C}$  for 4 h. This process results in the oxidation of  $\sim 1000\text{ }\text{\AA}$  of the exposed  $\text{In}_{0.5}(\text{Al}_{0.9}\text{Ga}_{0.1})_{0.5}\text{P}$  upper confining layer. The oxide formed is smooth and shiny with a uniform dark blue color, and is free of any observable pinholes. The  $\text{Si}_3\text{N}_4$  masking stripes are then removed in a  $\text{CF}_4$  plasma. The native oxide is unaffected by this treatment. The samples are next lapped to a thickness of  $\sim 125\text{ }\mu\text{m}$ , polished, metallized with Au-Zn-Au for contact to the  $p$ -type side and with Ge-Ni-Au for the  $n$ -type side, alloyed, cleaved into bars  $\sim 375\text{ }\mu\text{m}$  in length, and are sawed into individual devices. We note that the metallization adheres well to the native oxide, allowing the saw cuts to be made directly on the metallized oxide. This is in contrast to deposited films which require the metals to be photolithographically lifted off in the areas to be sawed to prevent peeling during the sawing process. The excellent adhesion of the metallization suggests less stress is present in the oxide films and permits better heat sinking than with deposited dielectrics.

Figure 1 shows a scanning electron microscope (SEM) image of a stained cross section of the crystal before removal of the  $\text{Si}_3\text{N}_4$  masking stripe. The oxide [Fig. 1(b)] is  $\sim 1000\text{ }\text{\AA}$  thick and is uniform across the wafer surface. Additionally, the oxide grows up to the edge of and slightly undercuts the contact stripe [Fig. 1(a)], resulting in complete isolation of the noncontacted areas.

The insulating properties of the oxide are demonstrated in the current-voltage ( $I$ - $V$ ) characteristics of Fig. 2. The  $I$ - $V$  characteristic of a diode prepared in the contact region [corresponding to the (a) region of Fig. 1] is shown in Fig. 2(a). The diode exhibits typical characteristics with "turn-on" of conduction at  $\sim 1.6\text{ V}$  and a forward resistance of  $\sim 5\text{ }\Omega$ . To check the current-blocking characteristics of the oxide, devices are also sawed with no contact stripe regions present. These devices [corresponding to

<sup>a)</sup>AT & T Doctoral Fellow.

<sup>b)</sup>Supported by Wright Laboratory/Material Directorate.

<sup>c)</sup>Now at Amoco Technology Company, Amoco Research Center, Naperville, Illinois 60566.

# Native-oxide-masked Si impurity-induced layer disordering of $\text{Al}_x\text{Ga}_{1-x}\text{As}-\text{Al}_y\text{Ga}_{1-y}\text{As}-\text{Al}_z\text{Ga}_{1-z}\text{As}$ quantum-well heterostructures

N. El-Zein, N. Holonyak, Jr., F. A. Kish,<sup>a)</sup> A. R. Sugg, T. A. Richard, and J. M. Dallesasse<sup>b)</sup>  
*Electrical Engineering Research Laboratory, Center for Compound Semiconductor Microelectronics,  
and Materials Research Laboratory, University of Illinois at Urbana-Champaign, Urbana,  
Illinois 61801*

S. C. Smith and R. D. Burnham

*Amoco Technology Company, Amoco Research Center, Naperville, Illinois 60566*

(Received 18 April 1991; accepted for publication 17 May 1991)

Data are presented showing that the native oxide that can be formed on high Al composition  $\text{Al}_x\text{Ga}_{1-x}\text{As}$  ( $x \geq 0.7$ ) confining layers commonly employed on  $\text{Al}_x\text{Ga}_{1-x}\text{As}-\text{Al}_y\text{Ga}_{1-y}\text{As}-\text{Al}_z\text{Ga}_{1-z}\text{As}$  ( $y > z$ ) superlattices or quantum-well heterostructures serves as an effective mask against Si diffusion, and thus impurity-induced layer disordering. The high-quality native oxide is produced by the conversion of high-composition  $\text{Al}_x\text{Ga}_{1-x}\text{As}$  ( $x \geq 0.7$ ) confining layers via  $\text{H}_2\text{O}$  vapor oxidation ( $\geq 400^\circ\text{C}$ ) in  $\text{N}_2$  carrier gas.

## I. INTRODUCTION

High-composition  $\text{Al}_x\text{Ga}_{1-x}\text{As}$  ( $x \geq 0.7$ ) layers may be unstable in normal room environmental conditions ( $20\text{--}25^\circ\text{C}$ , varying humidity) because of destructive hydrolyzation.<sup>1,2</sup> This is more of a problem for thicker layers ( $\geq 0.1\ \mu\text{m}$ ) of higher alloy composition ( $x \geq 0.7$ ) and less of a problem for thinner layers ( $\leq 100\ \text{\AA}$ ), even at high compositions. This instability is of major concern for various device applications employing high-gap  $\text{Al}_x\text{Ga}_{1-x}\text{As}$ , e.g., higher-composition thick confining layers on quantum-well heterostructures (QWHs) or on superlattices (SLs). Recently, in an attempt to accelerate the destructive hydrolyzation process for further study, we have formed stable native oxides from high-composition  $\text{Al}_x\text{Ga}_{1-x}\text{As}$  (Ref. 3) by reaction with  $\text{H}_2\text{O}$  vapor (in an  $\text{N}_2$  carrier gas) at elevated temperatures ( $\geq 400^\circ\text{C}$ ). We mention that higher-temperature oxidation is important for the formation of stable, device-quality Al-bearing oxides (compared to generally poorer suboxides formed at lower temperatures).<sup>4</sup> Native oxides formed on  $\text{Al}_x\text{Ga}_{1-x}\text{As}$  can serve as excellent insulators and have proved to be useful in device applications.<sup>5,6</sup> Development of more sophisticated devices utilizing the native  $\text{Al}_x\text{Ga}_{1-x}\text{As}$  oxide require the oxide to mask impurity diffusion, e.g., for definable or patterned impurity-induced layer disordering (IILD).<sup>7</sup> The masking capability of the native  $\text{Al}_x\text{Ga}_{1-x}\text{As}$  oxide for IILD Zn diffusion (Zn vapor,  $\sim 600^\circ\text{C}$ ) has been previously demonstrated.<sup>8</sup> In many cases, it is more important to be able to perform donor diffusion (Si) and realize IILD in a patterned (maskable) form. This generally requires higher temperatures ( $\sim 800^\circ\text{C}$ ) and frequently solid sources, as well as sometimes vapor sources. In this paper we demonstrate the capability of the native  $\text{Al}_x\text{Ga}_{1-x}\text{As}$  oxide to mask diffusion and IILD from a Si solid source. Scanning electron microscopy (SEM), shallow-angle beveled cross sections, and photoluminescence measurements are used to

demonstrate the oxide masking of Si diffusion (solid-source diffusion), and thus patterned IILD.

## II. EXPERIMENTAL PROCEDURE

Both superlattice (SL) and single-quantum-well-heterostructure (QWH) crystals are employed in the present work. The SLs and QWHs are grown on (100) GaAs substrates by metalorganic chemical vapor deposition (MOCVD) as described extensively elsewhere.<sup>9</sup> One SL (designated SL1) consists of 20 GaAs wells ( $L_z \sim 500\ \text{\AA}$ ) and 21  $\text{Al}_{0.5}\text{Ga}_{0.5}\text{As}$  barriers ( $L_B \sim 500\ \text{\AA}$ ) that are confined on the upper and lower sides with  $\sim 1000\ \text{\AA}$  of  $\text{Al}_{0.8}\text{Ga}_{0.2}\text{As}$ . Another SL (designated SL2) consists of 15 GaAs wells ( $L_z \sim 335\ \text{\AA}$ ) and 16  $\text{Al}_{0.5}\text{Ga}_{0.5}\text{As}$  barriers ( $L_B \sim 335\ \text{\AA}$ ) confined with  $\sim 1000\ \text{\AA}$  of  $\text{Al}_{0.6}\text{Ga}_{0.4}\text{As}$  on both sides. On top of the upper confining layer of SL2 is a  $500\text{-\AA}$   $\text{Al}_x\text{Ga}_{1-x}\text{As}$  linearly graded region (from  $x=0$  to  $0.85$ ) followed by a  $\text{Al}_{0.85}\text{Ga}_{0.15}\text{As}$  cap layer ( $0.1\ \mu\text{m}$ ). Both SL crystals are undoped. The QWH crystal employed here (which is useful for QWH lasers) consists of an  $n$ -type GaAs buffer layer, followed by a  $\sim 1\text{-}\mu\text{m}$   $n$ -type  $\text{Al}_{0.8}\text{Ga}_{0.2}\text{As}$  lower confining layer, an undoped  $\sim 2000\text{-\AA}$   $\text{Al}_{0.25}\text{Ga}_{0.75}\text{As}$  waveguide region, a  $\sim 0.9\text{-}\mu\text{m}$   $p$ -type  $\text{Al}_{0.8}\text{Ga}_{0.2}\text{As}$  upper confining layer, and a heavily doped  $p$ -type GaAs cap ( $\sim 800\ \text{\AA}$ ) layer on top. In the center of the waveguide region is an undoped  $200\text{-\AA}$   $\text{Al}_{0.06}\text{Ga}_{0.94}\text{As}$  quantum well.

Oxidation of the wafers is performed at  $400^\circ\text{C}$  in a "wet" atmosphere ( $\text{N}_2 + \text{H}_2\text{O}$  vapor) in an open-tube furnace. The "wet" atmosphere is provided by flowing an  $\text{N}_2$  carrier gas ( $1.5\ \text{scfh}$ ) through an  $\text{H}_2\text{O}$  bubbler maintained at  $95^\circ\text{C}$ .<sup>3</sup> Since both SL samples are not capped, they are immediately subjected to oxidation after the crystal growth to prevent destructive atmospheric hydrolyzation.<sup>4</sup> Superlattice 1 (SL1) is oxidized for 3 h, and SL2 for only 1 h.

<sup>a)</sup>AT&T Doctoral Fellow.

<sup>b)</sup>Current address: Amoco Technology Company, Amoco Research Center, Naperville, Illinois 60566.

# Planar native-oxide index-guided $\text{Al}_x\text{Ga}_{1-x}\text{As}$ -GaAs quantum well heterostructure lasers

F. A. Kish,<sup>a)</sup> S. J. Caracci,<sup>b)</sup> N. Holonyak, Jr., J. M. Dallesasse,<sup>c)</sup> K. C. Hsieh,  
and M. J. Ries

*Electrical Engineering Research Laboratory, Center for Compound Semiconductor Microelectronics, and  
Materials Research Laboratory, University of Illinois at Urbana-Champaign, Urbana, Illinois  
61801*

S. C. Smith and R. D. Burnham

*Amoco Technology Company, Amoco Research Center, Naperville, Illinois 60566*

(Received 19 April 1991; accepted for publication 11 July 1991)

A new form of planar index-guided laser diode is demonstrated with a relatively thick ( $\sim 0.4 \mu\text{m}$ ) native oxide employed to define the lateral optical waveguide (transverse to the laser stripe). Oxidation of high-gap  $\text{Al}_x\text{Ga}_{1-x}\text{As}$  in a "wet" ambient results in the transformation of most of the upper confining layer to a lower-index current-blocking native oxide outside of the active stripe. Planar quantum well heterostructure (QWH)  $\text{Al}_x\text{Ga}_{1-x}\text{As}$ -GaAs laser diodes fabricated by this process exhibit both optical and current confinement. Continuous 300 K threshold currents as low as 10 mA (uncracked facets) and kink-free single-longitudinal-mode operation are demonstrated for  $\sim 2\text{-}\mu\text{m}$ -wide active region devices.

The fabrication of high-performance laser diodes requires a means of providing both optical and current confinement in order to limit current spreading, define current paths, and form optical waveguides.<sup>1</sup> Recently a new technique has been demonstrated to fabricate stripe-geometry gain-guided laser diodes by the formation of a thin ( $\sim 1000 \text{ \AA}$ ) current-blocking high-gap  $\text{Al}_x\text{Ga}_{1-x}\text{As}$  native oxide outside of the laser stripe.<sup>2,3</sup> In this letter oxidation of most of the high-gap  $\text{Al}_x\text{Ga}_{1-x}\text{As}$ <sup>2</sup> upper confining layer of an  $\text{Al}_x\text{Ga}_{1-x}\text{As}$ -GaAs quantum well heterostructure (QWH) laser (outside of the active stripe) is employed to form a low-index current-blocking native oxide. The resulting planar index-guided devices exhibit both optical and current confinement as well as kink-free single-longitudinal-mode operation. Additionally, these lasers (fabricated on moderately low-threshold QWH crystals) have 300 K continuous (cw) thresholds as low as 10 mA for a  $\sim 2\text{-}\mu\text{m}$ -wide active stripe.

The QWH crystal employed in this work is grown (on  $n$ -type GaAs) by metalorganic chemical vapor deposition (MOCVD).<sup>4</sup> The epitaxial layers of interest are a  $\sim 1 \mu\text{m}$   $\text{Al}_{0.77}\text{Ga}_{0.23}\text{As}$   $n$ -type lower confining layer, a  $\sim 1400 \text{ \AA}$  undoped  $\text{Al}_{0.3}\text{Ga}_{0.7}\text{As}$  waveguide region, a  $\sim 0.5 \mu\text{m}$   $\text{Al}_{0.8}\text{Ga}_{0.2}\text{As}$   $p$ -type upper confining layer, and a  $\sim 800 \text{ \AA}$  heavily doped  $p$ -type GaAs cap. A  $\sim 100 \text{ \AA}$  GaAs quantum well (undoped) is grown in the center of the waveguide layer.

The laser fabrication begins with the deposition on the crystal of  $\sim 1000 \text{ \AA}$   $\text{Si}_3\text{N}_4$ , which is patterned with photoresist into two choices of stripe width (2 and  $8 \mu\text{m}$ ). These stripes serve as a mask for chemical etching of the GaAs contact layer, leaving the high-gap  $\text{Al}_{0.8}\text{Ga}_{0.2}\text{As}$  upper con-

fining layer exposed outside of the laser stripe. The crystal is then placed in an open-tube furnace (supplied with a  $\text{N}_2$  carrier gas bubbled through  $\text{H}_2\text{O}$  at  $95^\circ\text{C}$ ) at  $450^\circ\text{C}$  for  $\sim 30$  min. This process results in the transformation of almost the entire exposed confining layer to a native oxide. Next the  $\text{Si}_3\text{N}_4$  covering the contact stripe is removed, and the samples are Zn-diffused at  $540^\circ\text{C}$  for 30 min to improve the contacts. The crystals are then lapped and polished, metallized with Ti-Au for  $p$ -type contacts and Ge-Ni-Au for  $n$ -type contacts, cleaved into  $\sim 250\text{-}\mu\text{m}$ -wide bars, diced, and mounted on In-coated copper heat sinks.

Figure 1(a) shows a scanning electron microscope (SEM) image of a stained cross section of a  $\sim 2\text{-}\mu\text{m}$ -wide laser structure after oxidation (except for the active region) of almost the entire thickness ( $\sim 0.4 \mu\text{m}$ ) of the upper confining layer. The native oxide extends downward almost to the waveguide region (WG in Fig. 2). The oxidation process obviously undercuts the GaAs cap "masking" layer, thus, resulting in  $\sim 1.7\text{-}\mu\text{m}$ -wide active stripe embedded in native oxide. The native oxide exhibits excellent current-blocking properties and confines the current to the stripe region.<sup>4,5</sup> Additionally, the native oxide exhibits a much lower index of refraction (ellipsometer measurements,  $n = 1.50\text{--}1.60$ )<sup>5</sup> than the original upper confining layer ( $n \sim 3.1$ ). Thus, the index step ( $3.1\text{--}1.6$ ), over a significant thickness of the QWH, forms an optical waveguide in the lateral direction.

The effect of the optical waveguide is shown by the near-field (NF) pattern in the inset (b) of the  $\sim 2\text{-}\mu\text{m}$ -wide device of Fig. 1(a). The full width at half-maximum (FWHM) of the optical field (fundamental transverse mode) is  $1.7 \mu\text{m}$  at a cw 300 K current of 20 mA ( $I \sim 1.25 I_{th}$ ) and remains fixed over the entire operating range investigated ( $I \lesssim 3 I_{th}$ ). The NF FWHM agrees well with the active stripe width defined by the native oxide [Fig. 1(a)], and indicates that the lower refractive index of the native oxide in the upper confining layer is sufficient to

<sup>a)</sup>AT&T Doctoral Fellow.

<sup>b)</sup>Supported by Wright Laboratory/Materials Directorate.

<sup>c)</sup>Present address: Amoco Technology Company, Amoco Research Center, Naperville, Illinois 60566.

# Native-oxide coupled-cavity $\text{Al}_x\text{Ga}_{1-x}\text{As}$ -GaAs quantum well heterostructure laser diodes

N. El-Zein, F. A. Kish,<sup>a)</sup> N. Holonyak, Jr., A. R. Sugg, and M. J. Ries  
*Electrical Engineering Research Laboratory, Center for Compound Semiconductor Microelectronics,  
 and Materials Research Laboratory, University of Illinois at Urbana-Champaign,  
 Urbana, Illinois 61801*

S. C. Smith, J. M. Dallesasse, and R. D. Burnham  
*Amoco Technology Company, Amoco Research Center, Naperville, Illinois 60566*

(Received 9 August 1991; accepted for publication 23 September 1991)

Data are presented demonstrating  $\text{Al}_x\text{Ga}_{1-x}\text{As}$ -GaAs quantum well heterostructure laser diodes consisting of an array of coupled cavities (19  $\mu\text{m}$  long on 22  $\mu\text{m}$  centers,  $\sim 250 \mu\text{m}$  total length) arranged lengthwise in single 10- $\mu\text{m}$ -wide laser stripes. The cavities are defined by a native oxide formed from a significant portion of the high-gap  $\text{Al}_x\text{Ga}_{1-x}\text{As}$  upper confining layer. The native oxide (grown at 425 °C in  $\text{H}_2\text{O}$  vapor +  $\text{N}_2$  carrier gas) confines the injected carriers and optical field within the cavities, resulting in reflection and optical feedback distributed periodically along the laser stripe. These diodes exhibit single-longitudinal-mode operation over an extended range (relative to similar diodes fabricated without multiple cavities). At high current injection levels, longitudinal-mode spectra demonstrate unambiguously oscillation from the internal coupled cavities.

The high gain required for oscillation in semiconductor lasers results in a large optical bandwidth in which laser operation is possible. This large bandwidth generally results in multiple-longitudinal-mode operation. For many applications, single-longitudinal-mode operation is required. Consequently, sophisticated structures such as the distributed feedback (DFB) laser<sup>1</sup> and the cleaved-coupled-cavity ( $\text{C}^3$ ) laser<sup>2</sup> have been developed to insure single-mode operation. These devices operate by reflecting the electromagnetic wave within the laser stripe to lock the laser mode. The DFB laser employs a fine-scale periodic corrugation of relatively small index steps to interact with the electromagnetic wave. The  $\text{C}^3$  laser relies on several large-scale nonperiodic monolithic cavities for feedback and mode selection. In this letter, we describe  $\text{Al}_x\text{Ga}_{1-x}\text{As}$ -GaAs quantum well heterostructure (QWH) laser diodes utilizing large periodic index steps to couple multiple cavities (19  $\mu\text{m}$  long on 22  $\mu\text{m}$  centers,  $\sim 250 \mu\text{m}$  total length) arranged lengthwise along a single 10- $\mu\text{m}$ -wide laser stripe. The index step is provided by "wet" oxidation ( $\text{H}_2\text{O}$  vapor +  $\text{N}_2$  carrier gas, 425 °C) of the high-gap  $\text{Al}_x\text{Ga}_{1-x}\text{As}$  (Ref. 3) upper confining layer outside of the laser cavities. This native oxide possesses a low refractive index ( $n = 1.60$ ) (Ref. 4) and excellent insulating characteristics,<sup>5</sup> thus confining the injected carriers and making possible reflections between the multiple cavities. The coupling of the optical wave between cavities results in an increased range of single-longitudinal-mode operation ( $\sim I_{\text{th}}$  to  $\sim 4I_{\text{th}}$ ,  $I_{\text{th}}$  = threshold current). At higher injection currents the longitudinal-mode spacing corresponds to laser operation from a 38  $\mu\text{m}$  internal cavity ( $2 \times 19 \mu\text{m}$ ), indicating that the native oxide provides sufficient reflection of the optical wave for laser oscillation.

The QWH laser crystal employed in this work is grown on an  $n$ -type GaAs substrate by metalorganic chemical vapor deposition (MOCVD).<sup>6</sup> The growth begins with  $n$ -type buffer layers of GaAs ( $\sim 0.5 \mu\text{m}$ ) and  $\text{Al}_{0.23}\text{Ga}_{0.77}\text{As}$  ( $\sim 1.0 \mu\text{m}$ ). These are followed by a  $\sim 1.5 \mu\text{m}$   $n$ -type  $\text{Al}_{0.3}\text{Ga}_{0.5}\text{As}$  lower confining layer, a  $\sim 2100 \text{ \AA}$  undoped  $\text{Al}_{0.23}\text{Ga}_{0.77}\text{As}$  waveguide region, a  $\sim 3500 \text{ \AA}$   $p$ -type  $\text{Al}_{0.8}\text{Ga}_{0.2}\text{As}$  upper confining layer, and a  $\sim 800 \text{ \AA}$  heavily doped  $p$ -type GaAs contact layer. A  $\sim 100 \text{ \AA}$  undoped GaAs quantum well (QW) is grown inside of the waveguide region  $\sim 700 \text{ \AA}$  from the lower confining layer. The position of the QW is displaced from the center of the waveguide for more effective overlap of the high-gain region with the optical mode, which is displaced towards the substrate due to the asymmetric confining layers. This asymmetry is purposely introduced to minimize the effects of the surface of the laser crystal (located  $\sim 3500 \text{ \AA}$  from the waveguide) by shifting the optical field toward the substrate. The shallow upper confining layer is desirable in order to minimize current spreading, allow finer pattern definition, and improved heat dissipation with the crystal mounted  $p$  side "down" and thus the active region closer to the heat sink.

The laser diode fabrication begins with deposition of  $\sim 1000 \text{ \AA}$  of  $\text{Si}_3\text{N}_4$  on the crystal surface which is then patterned into repeated (masked) rectangular cavities (19  $\mu\text{m}$  long on 22  $\mu\text{m}$  centers, 10  $\mu\text{m}$  wide) arranged lengthwise in stripes. The  $\text{Si}_3\text{N}_4$  masks the GaAs contact layer from chemical etching ( $\text{H}_2\text{SO}_4\text{:H}_2\text{O}_2\text{:H}_2\text{O}$ , 1:8:80), leaving the  $\text{Al}_{0.8}\text{Ga}_{0.2}\text{As}$  upper confining layer exposed outside of the patterned cavities. The sample is next placed in an open tube furnace, supplied with  $\text{H}_2\text{O}$  vapor in an  $\text{N}_2$  carrier gas, at 425 °C for 20 min. This process results in the transformation of  $\sim 1300 \text{ \AA}$  of the  $\text{Al}_{0.8}\text{Ga}_{0.2}\text{As}$  upper confining layer to native oxide outside of the repeated cavities. The  $\text{Si}_3\text{N}_4$  is subsequently removed in a  $\text{CF}_4$  plasma. Figure 1

<sup>a)</sup>AT&T Doctoral Fellow.

# Visible spectrum native-oxide coupled-stripe $\text{In}_{0.5}(\text{Al}_x\text{Ga}_{1-x})_{0.5}\text{P}-\text{In}_{0.5}\text{Ga}_{0.5}\text{P}$ quantum well heterostructure laser arrays

F. A. Kish,<sup>a)</sup> S. J. Caracci, N. Holonyak, Jr. and S. A. Maranowski  
Electrical Engineering Research Laboratory, Center for Compound Semiconductor Microelectronics,  
and Materials Research Laboratory, University of Illinois at Urbana-Champaign, Urbana, Illinois 61801

J. M. Dallesasse, R. D. Burnham, and S. C. Smith  
Amoco Technology Company, Amoco Research Center, Naperville, Illinois 60566

(Received 26 August 1991; accepted for publication 23 September 1991)

Data are presented demonstrating the continuous (cw) operation (10–50 °C) of coupled-stripe  $\text{In}_{0.5}(\text{Al}_x\text{Ga}_{1-x})_{0.5}\text{P}-\text{In}_{0.5}\text{Ga}_{0.5}\text{P}$  multiple quantum well heterostructure (QWH) visible ( $\lambda \sim 655$  nm) laser arrays. The ten stripe QWH arrays (3  $\mu\text{m}$  emitters on 4  $\mu\text{m}$  centers) are defined by "wet" oxidation ( $\text{H}_2\text{O}$  vapor in  $\text{N}_2$  carrier gas, 550 °C) of the high gap  $\text{In}_{0.5}(\text{Al}_x\text{Ga}_{1-x})_{0.5}\text{P}$  upper confining layer outside of the active stripes. The gain-guided arrays exhibit relatively low cw 20 °C threshold current densities ( $\sim 1.6$  kA/cm<sup>2</sup>,  $\sim 450$   $\mu\text{m}$  cavity) and high output powers of 25 mW per uncoated facet (cw, 20 °C). Optical coupling between stripes results in a near diffraction-limited single-lobe far-field pattern indicative of oscillation in the lowest order supermode of the array (in-phase operation).

The observation of stimulated emission in  $\text{GaAs}_{1-x}\text{P}_x$  diodes,<sup>1</sup> followed by  $\text{Al}_x\text{Ga}_{1-x}\text{As}$ <sup>2,3</sup> and then  $\text{In}_y\text{Ga}_{1-y}\text{P}$ ,<sup>4,5</sup> demonstrated quite early the feasibility of visible spectrum semiconductor lasers. The capacity of substituting Al for Ga to form higher gap lattice-matched heterostructures via metalorganic chemical vapor deposition (MOCVD)<sup>6</sup> has led, in the  $\text{In}_y\text{Ga}_{1-y}\text{P}$  system, to the further capability of producing high-quality visible-wavelength  $\text{In}_y(\text{Al}_x\text{Ga}_{1-x})_y\text{P}$  quantum well heterostructure laser material lattice-matched ( $y \sim 0.5$ ) to GaAs. These developments have resulted in short wavelength,<sup>7,8</sup> high-power,<sup>9,10</sup> and high reliability<sup>11</sup> visible spectrum laser diodes. However, little work has been concentrated on visible spectrum coupled-stripe arrays, which provide the advantage of delivering high output powers in a narrow beam. In this letter we present data demonstrating high power [25 mW per uncoated facet, 20 °C, continuous wave (cw)] coupled-stripe  $\text{In}_{0.5}(\text{Al}_x\text{Ga}_{1-x})_{0.5}\text{P}-\text{In}_{0.5}\text{Ga}_{0.5}\text{P}$  multiple quantum well heterostructure (QWH) laser arrays operating in the visible spectrum,  $\lambda \sim 655$  nm. The ten stripe arrays are defined by conversion of the high-gap  $\text{In}_{0.5}(\text{Al}_x\text{Ga}_{1-x})_{0.5}\text{P}$  upper confining layer outside of the active stripes to native oxide (formed at 550 °C in  $\text{H}_2\text{O}$  vapor +  $\text{N}_2$  carrier gas).<sup>12,13</sup>

The quantum well heterostructure (QWH) crystal employed in this work is grown by MOCVD on an  $n$ -type GaAs:Si substrate. The  $\text{In}_{0.5}(\text{Al}_x\text{Ga}_{1-x})_{0.5}\text{P}$  epitaxial layers consist of a  $\sim 1.0$   $\mu\text{m}$   $n$ -type lower confining layer ( $x \sim 0.9$ ), a multiple quantum well active region confined by  $\sim 750$  Å linearly graded ( $x \sim 0.9 \leftrightarrow x \sim 0.3$ ) regions, a  $\sim 1.0$   $\mu\text{m}$   $p$ -type upper confining layer ( $x \sim 0.9$ ), a  $p$ -type ( $x \sim 0$ ) cap layer, and a heavily Zn-doped GaAs contact layer. The active region consists of four 100 Å quantum wells ( $x \sim 0$ ) separated by three 200 Å barriers ( $x \sim 0.3$ ). A four well structure is employed since previous work has shown that a similar design provides relatively high-performance short-wavelength operation.<sup>7</sup>

Laser diode fabrication begins by patterning 1000-Å thick  $\text{Si}_3\text{N}_4$  into arrays of ten 3- $\mu\text{m}$  wide stripes (on 4  $\mu\text{m}$  centers) and, for comparison, 10- $\mu\text{m}$  wide single stripes on the samples. These stripes serve as a mask for the chemical etching (Br-methanol, 0.1%) of the capping layers, leaving the high-gap  $\text{In}_{0.5}(\text{Al}_{0.9}\text{Ga}_{0.1})_{0.5}\text{P}$  exposed outside of the active stripes. The  $\text{Si}_3\text{N}_4$  also serves to prevent degradation of the contact layer during the oxidation process. The crystals are then placed in an open tube furnace (550 °C, 1 h) supplied with  $\text{H}_2\text{O}$  vapor in a  $\text{N}_2$  carrier gas. This procedure results in the conversion of the exposed high-gap  $\text{In}_{0.5}(\text{Al}_{0.9}\text{Ga}_{0.1})_{0.5}\text{P}$  to  $\sim 1000$  Å of a current-blocking native oxide.<sup>13</sup> The  $\text{Si}_3\text{N}_4$  (on the active stripes) is next removed in a  $\text{CF}_4$  plasma, and the samples are lapped and polished to a thickness of  $\sim 125$   $\mu\text{m}$ . The crystals are metallized with Au-Zn-Au for the  $p$ -type contacts and Ge-Ni-Au for  $n$ -type contact, and then are cleaved, diced, and mounted  $p$ -side down on In-coated copper heat sinks.

In order to assess the quality of the QWH material, 10- $\mu\text{m}$  wide native-oxide single-stripe lasers have been fabricated for comparison. Typical cw 20 °C performance of a 10  $\mu\text{m}$  single stripe laser diode is shown in Fig. 1. The light versus current ( $L-I$ ) curve shows a threshold current of 96 mA (uncoated facets, 305  $\mu\text{m}$  cavity), corresponding to a current density of 3.1 kA/cm<sup>2</sup> (uncorrected for current spreading). The total external differential quantum efficiency ( $\eta$ ) is 42% up to 1.5 mW, and the maximum output power is thermally limited to 5 mW per facet. The diode lases with multiple longitudinal modes, with the primary mode at  $\lambda \approx 6523$  Å (inset Fig. 1). We attribute the multimode operation to the weakly coupled four-well form of the QWH crystal, which makes each well in essence a separate laser. Despite the relatively high threshold current density, these lasers show no signs of degradation after hours of testing.

Continuous operation of a ten stripe coupled array (3  $\mu\text{m}$  emitters on 4  $\mu\text{m}$  centers) stabilized (on a thermoelec-

<sup>a)</sup>AT&T Doctoral Fellow.

# Coupled-stripe in-phase operation of planar native-oxide index-guided $\text{Al}_y\text{Ga}_{1-y}\text{As-GaAs-In}_x\text{Ga}_{1-x}\text{As}$ quantum-well heterostructure laser arrays

F. A. Kish,<sup>a)</sup> S. J. Caracci, and N. Holonyak, Jr.

Electrical Engineering Research Laboratory, Center for Compound Semiconductor Microelectronics,  
and Materials Research Laboratory, University of Illinois at Urbana-Champaign, Urbana,  
Illinois 61801

P. Gavrilovic, K. Meehan, and J. E. Williams

Microelectronics Laboratory, Polaroid Corporation, Cambridge, Massachusetts 02139

(Received 15 July 1991; accepted for publication 15 October 1991)

High-performance, coupled-stripe, planar, index-guided  $\text{Al}_y\text{Ga}_{1-y}\text{As-GaAs-In}_x\text{Ga}_{1-x}\text{As}$  quantum-well heterostructure (QWH) laser arrays are fabricated by the formation of a relatively thick, current-blocking, native oxide from the high-gap  $\text{Al}_y\text{Ga}_{1-y}\text{As}$  upper confining layer between active stripes. Precise control of the thickness of the native oxide layer between emitters provides a means of varying the index step between stripes, and permits tailoring of the optical profile to produce in-phase operation. The 10-stripe coupled QWH laser arrays ( $\sim 3\text{-}\mu\text{m}$ -wide stripes on  $4\text{-}\mu\text{m}$  centers) exhibit near-diffraction-limited, single-lobed, far-field patterns with low continuous (cw) thresholds ( $\sim 45\text{ mA}$ ) and cw output powers (total external differential quantum efficiency  $> 50\%$ ) of over 100 mW per uncoated facet.

Coupled-stripe laser-diode arrays offer the possibility of obtaining high output powers with decreased beam divergence and single-longitudinal mode operation. In addition, index-guided arrays, compared to their gain-guided counterparts, are preferred due to increased mode stability and coherence, and decreased beam astigmatism. Several methods have been employed to fabricate index-guided arrays, including: channel etching,<sup>1,2</sup> epitaxial regrowth<sup>3</sup> or overgrowth,<sup>4</sup> and impurity-induced layer disordering (IILD).<sup>5-7</sup> Many of these techniques require relatively sophisticated processing and/or provide limited control of the index step between emitters. Precise adjustment of the index step permits control of the optical field between emitters, and thus, control of the coupling between stripes. This coupling dramatically affects the far-field radiation patterns, determining the supermode(s) in which the array will oscillate.

Recently, we have introduced a new form of planar, index-guided laser diode with optical and current confinement provided by the conversion of most of the high-gap  $\text{AlGaAs}$  upper confining layer to a lower-index ( $n \approx 1.60$ ) current-blocking native oxide (outside of the active stripe).<sup>8</sup> By simply adjusting the thickness of the native oxide outside of the active stripe, we are able to control simultaneously both the optical field and the gain profile. In this letter, we utilize this process to produce coupled-stripe, planar, native-oxide, index-guided  $\text{Al}_y\text{Ga}_{1-y}\text{As-GaAs-In}_x\text{Ga}_{1-x}\text{As}$  quantum-well heterostructure (QWH) laser arrays operating in-phase ( $0^\circ$  phase shift between emitters). These 10-stripe arrays ( $\sim 3\text{-}\mu\text{m}$ -wide emitters on  $4\text{-}\mu\text{m}$  centers) exhibit near diffraction-limited, single-lobe, far-field patterns with low continuous (cw) threshold currents ( $\sim 45\text{ mA}$ ) and cw output powers of  $> 100\text{ mW}$  per uncoated facet.

The QWH crystal employed in this work is grown by

low-pressure metalorganic chemical vapor deposition (MOCVD) as described extensively elsewhere.<sup>7,9</sup> The crystal is grown on an  $n$ -type GaAs substrate at  $800^\circ\text{C}$ , except the  $\text{In}_x\text{Ga}_{1-x}\text{As}$  QW, which is grown at  $630^\circ\text{C}$  to prevent In desorption from the crystal surface. The growth begins with an  $n$ -type GaAs buffer layer, followed by an  $\sim 1.25\text{-}\mu\text{m}$   $\text{Al}_{0.8}\text{Ga}_{0.2}\text{As}$   $n$ -type confining layer, an  $\sim 3000\text{ \AA}$  undoped active region, an  $\sim 0.6\text{-}\mu\text{m}$   $\text{Al}_{0.8}\text{Ga}_{0.2}\text{As}$   $p$ -type upper confining layer, and a heavily doped  $p$ -type GaAs contact layer ( $\sim 1000\text{ \AA}$ ). The active region consists of an outer  $\text{Al}_{0.3}\text{Ga}_{0.7}\text{As}$  waveguide (WG) with an  $\sim 100\text{ \AA}$   $\text{In}_{0.1}\text{Ga}_{0.9}\text{As}$  QW in its center, confined by an  $\sim 320\text{ \AA}$  GaAs spacer layer on each side. We note that this structure is a high-confinement structure designed for low-threshold operation. Higher output powers may be realized by employing an alternative lower confinement structure (e.g., lower composition confining layers and a thinner waveguide region).

Two different sets of laser-diode arrays are fabricated by patterning  $\sim 1000\text{ \AA}$  of  $\text{Si}_3\text{N}_4$  into a 10-stripe array of  $3\text{-}\mu\text{m}$ -wide stripes on  $4\text{-}\mu\text{m}$  center-to-center spacings. The exposed GaAs cap (outside of the masking stripes) is then removed by chemical etching ( $\text{H}_2\text{SO}_4\text{:H}_2\text{O}_2\text{:H}_2\text{O}$ , 1:8:80) and the crystal is placed in an open-tube furnace (supplied with a  $\text{N}_2$  carrier gas bubbled through  $\text{H}_2\text{O}$  at  $\sim 95^\circ\text{C}$ ) at  $450^\circ\text{C}$ . One sample (index guided) is oxidized for 50 min, resulting in the conversion of  $\sim 0.4\text{-}\mu\text{m}$  of the  $\text{Al}_{0.8}\text{Ga}_{0.2}\text{As}$  upper confining layer to native oxide. A second comparison set of gain-guided devices is fabricated by the formation of a thin ( $\sim 1000\text{ \AA}$ ) native oxide ( $450^\circ\text{C}$ , 15 min). The native oxide possesses excellent current-blocking properties and a lower refractive index ( $n \approx 1.60$ ), and thus simultaneously confines the current and optical field in the active stripe regions for sufficiently deep oxides.<sup>8</sup> Following oxidation, the  $\text{Si}_3\text{N}_4$  masking stripes are removed in a  $\text{CF}_4$  plasma and the crystals are Zn diffused at  $540^\circ\text{C}$  for 20 min to increase the doping in the stripe contact areas. The

<sup>a)</sup>AT&T Doctoral Fellow.

# Planar native-oxide buried-mesa $\text{Al}_x\text{Ga}_{1-x}\text{As-In}_{0.5}(\text{Al}_y\text{Ga}_{1-y})_{0.5}\text{P-In}_{0.5}(\text{Al}_z\text{Ga}_{1-z})_{0.5}\text{P}$ visible-spectrum laser diodes

F. A. Kish,<sup>a)</sup> S. J. Caracci, S. A. Maranowski, N. Holonyak, Jr.,  
and K. C. Hsieh

*Electrical Engineering Research Laboratory, Center for Compound Semiconductor Microelectronics, and  
Materials Research Laboratory, University of Illinois at Urbana-Champaign, Urbana, Illinois  
61801*

C. P. Kuo, R. M. Fletcher, T. D. Osentowski, and M. G. Craford  
*Hewlett Packard Company, Optoelectronics Division, San Jose, California 95131*

(Received 26 September 1991; accepted for publication 12 December 1991)

Data are presented demonstrating the continuous (cw) room-temperature (23 °C) operation of planar index-guided "buried-mesa"  $\text{Al}_x\text{Ga}_{1-x}\text{As-In}_{0.5}(\text{Al}_y\text{Ga}_{1-y})_{0.5}\text{P-In}_{0.5}\text{Ga}_{0.5}\text{P}$  heterostructure visible-spectrum laser diodes. The planar "mesa" structure is formed by "wet" oxidation ( $\text{H}_2\text{O}$  vapor +  $\text{N}_2$  carrier gas, 550 °C) of the  $\text{Al}_x\text{Ga}_{1-x}\text{As}$  on the composite  $\text{Al}_x\text{Ga}_{1-x}\text{As-In}_{0.5}(\text{Al}_y\text{Ga}_{1-y})_{0.5}\text{P}$  upper confining layer (outside of the active stripes). The oxidation process results in a  $\sim 0.5\text{-}\mu\text{m}$ -thick native oxide located (in depth) within  $\sim 3000$  Å of the active layer in the region outside of the laser stripes themselves. The oxide possesses excellent current-confinement properties and a low refractive index ( $n \approx 1.60$ ), resulting in relatively low-threshold laser operation for narrow-stripe devices. In addition, these devices exhibit transverse-mode confinement and small beam astigmatism because of the refractive index step provided by the deep native oxide.

## I. INTRODUCTION

The initial demonstration of stimulated emission in  $\text{In}_x\text{Ga}_{1-x}\text{P}$ ,<sup>1</sup> followed subsequently by the development of  $\text{In}_x\text{Ga}_{1-x}\text{P } p\text{-}n$  junction laser diodes,<sup>2</sup> has provided a basis for a system of III-V semiconductor laser lamps with possible wavelengths ranging from the green ( $\sim 5500$  Å) to the infrared ( $\sim 9000$  Å). Recent advances in crystal growth technology employing metalorganic chemical vapor deposition (MOCVD),<sup>3</sup> combined with Al-Ga substitution to form higher-gap heterostructures,<sup>4</sup> have resulted in a system of  $\text{In}_{0.5}(\text{Al}_y\text{Ga}_{1-y})_{0.5}\text{P}$  heterostructures lattice matched to GaAs. These developments have led to the achievement of continuous (cw) room-temperature operation of visible-spectrum  $\text{In}_{0.5}(\text{Al}_y\text{Ga}_{1-y})_{0.5}\text{P}$  laser diodes.<sup>5</sup> In addition, the lasing characteristics of these diodes have been improved (i.e., the device "geometry") to the point of transverse-mode stabilization.<sup>6-8</sup> These devices employ a "buried-mesa" geometry with transverse-mode confinement obtained with either complex<sup>6,7</sup> or real<sup>8</sup> refractive index steps. The mesa structures of previous reports are realized by multiple regrowth schemes, which unfortunately necessitate complex and cumbersome fabrication techniques.

In this paper we demonstrate planar index-guided "buried-mesa"  $\text{Al}_x\text{Ga}_{1-x}\text{As-In}_{0.5}(\text{Al}_y\text{Ga}_{1-y})_{0.5}\text{P-In}_{0.5}(\text{Al}_z\text{Ga}_{1-z})_{0.5}\text{P}$  double-heterostructure (DH) laser diodes fabricated by the relatively simple process of "wet" oxidation of the top-layer  $\text{Al}_x\text{Ga}_{1-x}\text{As}$ .<sup>9</sup> The "buried-mesa" structures, which are geometrically "flat" (planar), are formed by oxidation of the entire  $\sim 0.5\text{-}\mu\text{m}$   $\text{Al}_x\text{Ga}_{1-x}\text{As}$  layer (outside of the active stripe) on the

composite  $\text{Al}_x\text{Ga}_{1-x}\text{As-In}_{0.5}(\text{Al}_y\text{Ga}_{1-y})_{0.5}\text{P}$  upper confining layer. The oxide, which is located vertically within  $\sim 3000$  Å of the active region in the area outside of the laser stripe, provides both current and transverse-mode confinement by virtue of its current-blocking properties and low refractive index ( $n \approx 1.60$ ).<sup>10</sup> Consequently, low-threshold cw room-temperature (23 °C) operation is achieved in narrow-stripe devices that possess relatively small beam astigmatism because of the refractive index step provided by the deep native oxide.

## II. EXPERIMENTAL PROCEDURE

The laser crystals employed in this work are grown by MOCVD on  $n$ -type GaAs substrates. A schematic drawing of the crystal structures is shown in Fig. 1. The epitaxial layers of interest consist of a  $\sim 0.8\text{-}\mu\text{m}$   $n$ -type  $\text{In}_{0.5}(\text{Al}_{0.9}\text{Ga}_{0.1})_{0.5}\text{P}$  lower confining layer, followed by an undoped  $\text{In}_{0.5}(\text{Al}_z\text{Ga}_{1-z})_{0.5}\text{P}$  active region. Two different crystals are grown with the composition of the active region adjusted for recombination radiation at either  $\lambda \sim 660$  nm ( $z \sim 0$ ) or  $\lambda \sim 620$  nm ( $z \sim 0.2$ ). The growth of the top layers ( $p$  type) is continued with  $\sim 0.3$   $\mu\text{m}$  of  $\text{In}_{0.5}(\text{Al}_{0.9}\text{Ga}_{0.1})_{0.5}\text{P}$  followed by  $\sim 0.5$   $\mu\text{m}$  of  $\text{Al}_{0.4}\text{Ga}_{0.6}\text{As}$ , and then finished with the entire structure capped by a heavily doped  $p$ -type  $\sim 1000\text{-}\text{\AA}$  GaAs contact layer. A thin  $\sim 200\text{-}\text{\AA}$  spacer layer of  $\text{In}_{0.5}\text{Ga}_{0.5}\text{P}$  is grown between the  $\text{In}_{0.5}(\text{Al}_{0.9}\text{Ga}_{0.1})_{0.5}\text{P}$  and the  $\text{Al}_{0.4}\text{Ga}_{0.6}\text{As}$  layers (top layers). This layer serves to decrease the large valence-band offset between the  $\text{In}_{0.5}(\text{Al}_y\text{Ga}_{1-y})_{0.5}\text{P}$  and  $\text{Al}_x\text{Ga}_{1-x}\text{As}$  layers,<sup>6,11</sup> thus reducing the forward voltage drop across the layers. We note that the  $\text{Al}_x\text{Ga}_{1-x}\text{As}$  upper confining layer is employed as the source material from which high-quality thick native oxides are formed.<sup>12</sup> At-

<sup>a)</sup>AT&T Doctoral Fellow.



# Planar native-oxide $\text{Al}_x\text{Ga}_{1-x}\text{As}$ -GaAs quantum well heterostructure ring laser diodes

F. A. Kish,<sup>a)</sup> S. J. Caracci, S. A. Maranowski, and N. Holonyak, Jr.  
*Electrical Engineering Research Laboratory, Center for Compound Semiconductor Microelectronics,  
and Materials Research Laboratory, University of Illinois at Urbana-Champaign,  
Urbana, Illinois 61801*

S. C. Smith and R. D. Burnham  
*Amoco Technology Company, Amoco Research Center, Naperville, Illinois 60566*

(Received 13 November 1991; accepted for publication 27 January 1992)

Native-oxide planar  $\text{Al}_x\text{Ga}_{1-x}\text{As}$ -GaAs quantum well heterostructure ring laser diodes (25- $\mu\text{m}$ -wide annulus, 250- $\mu\text{m}$  inside diameter, 300- $\mu\text{m}$  outside diameter) are demonstrated. The curved cavities (full-ring, half-ring, and quarter-ring) are defined by native oxidation ( $\text{H}_2\text{O}$  vapor +  $\text{N}_2$  carrier gas, 450 °C) of the *entire* upper confining layer inside and outside of the annulus. The native oxide provides current confinement and a sufficiently large lateral index step, and thus photon confinement, to support laser oscillation along the ring. Half-ring laser diodes fabricated in a self-aligned geometry exhibit continuous wave (cw) 300-K thresholds as low as  $\sim 105$  mA ( $\sim 500$ - $\mu\text{m}$  circular cavity length), high total external differential quantum efficiencies ( $\sim 49\%$ ), and cw output powers of  $> 40$  mW.

In order to manipulate photons around a "chip," e.g., for optoelectronic integrated circuits (OEICs), a planar processing technology for III-V materials that permits the formation of large lateral index steps (for use in waveguides) is required. Recently  $\text{H}_2\text{O}$  vapor oxidation has been employed to selectively form high-quality native oxides from high composition  $\text{Al}_x\text{Ga}_{1-x}\text{As}$ .<sup>1</sup> These native oxides exhibit excellent current-blocking properties,<sup>2</sup> a low refractive index ( $n \approx 1.60$ ),<sup>3</sup> and can be made relatively thick (microns) to form large lateral index steps for use in waveguides.<sup>4,5</sup> In this letter we present data demonstrating the use of the  $\text{Al}_x\text{Ga}_{1-x}\text{As}$  native oxide to simply fabricate planar self-aligned  $\text{Al}_x\text{Ga}_{1-x}\text{As}$ -GaAs quantum well heterostructure (QWH) ring laser diodes. Other workers have demonstrated laser diodes with circular cavities,<sup>6-8</sup> but fabricated by complex crystal regrowth schemes or by employing nonplanar geometries. Both are inconvenient for sophisticated processing and OEICs. In the present work,  $\text{H}_2\text{O}$  vapor oxidation<sup>1</sup> (450 °C) of the high-gap  $\text{Al}_x\text{Ga}_{1-x}\text{As}$  upper confining layer inside and outside of the annulus results in the formation of a thick ( $\sim 0.6$   $\mu\text{m}$ ) low-index ( $n \approx 1.60$ ) native oxide, and thus large lateral index steps. Planar native-oxide half-ring  $\text{Al}_x\text{Ga}_{1-x}\text{As}$ -GaAs QWH laser diodes are constructed that exhibit continuous (cw) 300 K thresholds as low as  $\sim 105$  mA ( $\sim 500$ - $\mu\text{m}$  circular cavity length) and high total external differential quantum efficiencies ( $\sim 49\%$ ).

The QWH laser crystal employed in this work is grown by metalorganic chemical vapor deposition (MOCVD)<sup>9</sup> on an *n*-type GaAs substrate. The layers of interest consist of an *n*-type  $\text{Al}_{0.8}\text{Ga}_{0.2}\text{As}$  ( $\sim 1$   $\mu\text{m}$ ) lower confining layer, a  $\sim 1500$ - $\text{\AA}$  undoped  $\text{Al}_{0.23}\text{Ga}_{0.77}\text{As}$  waveguide region with a  $\sim 100$ - $\text{\AA}$  GaAs quantum well in the center, a  $\sim 0.6$ - $\mu\text{m}$  *p*-type  $\text{Al}_{0.8}\text{Ga}_{0.2}\text{As}$  upper confining layer, and a heavily doped *p*-type GaAs contact layer ( $\sim 800$   $\text{\AA}$ ).

The laser fabrication begins with the patterning of  $\sim 1000$   $\text{\AA}$  of  $\text{Si}_3\text{N}_4$  into rings [25- $\mu\text{m}$ -wide annulus, 250- $\mu\text{m}$  inside diameter (i.d.), 300- $\mu\text{m}$  outside diameter (o.d.)]. The  $\text{Si}_3\text{N}_4$  rings serve as a mask for the chemical etching ( $\text{H}_2\text{SO}_4\text{:H}_2\text{O}_2\text{:H}_2\text{O}$ , 1:8:80) of the contact layer, thus leaving the  $\text{Al}_x\text{Ga}_{1-x}\text{As}$  upper confining layer exposed inside and outside of the masked rings. The sample is then placed in an open tube furnace (supplied with  $\text{H}_2\text{O}$  vapor +  $\text{N}_2$ ) at 450 °C for 35 min. This process results in the conversion of the upper confining layer (where exposed) to a  $\sim 0.6$ - $\mu\text{m}$  lower index ( $n \approx 1.60$ ) native oxide.<sup>1,2,4</sup>

At the ring edges the oxide extends (downward) through the *entire* upper confining layer as shown by the scanning electron microscope (SEM) image (Fig. 1) of a stained cross section. The oxide is deeper at the ring edge than beyond (to the right in Fig. 1). This effect may be a result of changes in  $\text{H}_2\text{O}$  adsorption, O/H diffusion, or stress induced by the presence of the masking stripe. The oxide profile is fairly isotropic, however, extending laterally essentially to the same extent as it does in depth. This allows the formation of rings with an annulus width of  $\lesssim 2$   $\mu\text{m}$ . Transmission electron microscope (TEM) images of similarly oxidized crystals indicate that some oxidation ( $\sim 200$   $\text{\AA}$ ) of the underlying  $\text{Al}_{0.23}\text{Ga}_{0.77}\text{As}$  waveguide region occurs.<sup>10</sup> Thus, the low-index native oxide extends into the waveguide layer, creating large lateral index steps for sideways optical confinement and waveguiding. Calculations based on propagation in a four-layer slab waveguide<sup>11</sup> for this deep oxide edge indicate a lateral index step  $> 0.05$ . Half-ring structures with the native oxide located  $\sim 1000$   $\text{\AA}$  away from the waveguide result in an insufficient index step for ring oscillation (data not shown).

After the oxidation, the  $\text{Si}_3\text{N}_4$  masking rings are selectively removed in a  $\text{CF}_4$  plasma, resulting in a self-aligned geometry. The sample is then Zn-diffused (540 °C, 20 min), and metallized with Ti-Au for the *p*-type contact and

<sup>a)</sup>AT&T Doctoral Fellow.



## Dependence on doping type ( $p/n$ ) of the water vapor oxidation of high-gap $\text{Al}_x\text{Ga}_{1-x}\text{As}$

F. A. Kish,<sup>a)</sup> S. A. Maranowski, G. E. Höfler, N. Holonyak, Jr., S. J. Caracci, J. M. Dallesasse,<sup>b)</sup> and K. C. Hsieh

Electrical Engineering Research Laboratory, Center for Compound Semiconductor Microelectronics, and Materials Research Laboratory, University of Illinois at Urbana-Champaign, Urbana, Illinois 61801

(Received 10 February 1992; accepted for publication 7 April 1992)

The oxidation ( $\text{H}_2\text{O}$  vapor +  $\text{N}_2$  carrier gas, 425–525 °C) of high-gap  $\text{Al}_x\text{Ga}_{1-x}\text{As}$  of different doping types ( $p$  and  $n$ ) is characterized by oxide depth measurements utilizing scanning electron microscopy. The conductivity type is found to affect significantly the oxidation rate, with  $p$ -type samples oxidizing more rapidly than  $n$ -type samples. Classical oxidation theory is employed to explain these phenomena which are related to the position of the Fermi level in the samples.

The recent discovery of the capability to form device-quality, insulating, low-index ( $n \approx 1.60$ ), and potentially thick native oxides from high-gap  $\text{Al}_x\text{Ga}_{1-x}\text{As}$  via water vapor oxidation<sup>1</sup> has proved to be extremely useful in various applications. These uses include: diffusion masking,<sup>2,3</sup> crystal stabilization from atmospheric degradation,<sup>4</sup> device definition,<sup>5</sup> leakage current passivation,<sup>6</sup> formation of planar waveguides and index-guided lasers,<sup>7</sup> and the definition of internal reflectors for Fabry–Perot cavities.<sup>8</sup> An understanding of the factors influencing the oxidation rate is required for device processing, and, in addition, to better understand the water vapor oxidation mechanisms. In this letter we report on the water vapor oxidation of high-gap  $\text{Al}_x\text{Ga}_{1-x}\text{As}$  with different conductivity types. Oxide depth measurements obtained from scanning electron microscope (SEM) images of stained crystal cross sections show that the conductivity type ( $p$  or  $n$ ) affects significantly the oxidation rate. These phenomena are attributed to a dependence of the oxidation process on the position of the Fermi level in the crystal.

The crystals employed in these experiments are grown by metalorganic chemical vapor deposition (MOCVD)<sup>9</sup> on {100} semi-insulating (SI) GaAs substrates in an Emcore GS-3000 DFM reactor. The crystal growth precursors are trimethylgallium, trimethylaluminum, and arsine, and the  $n$  and  $p$  dopants are silane and carbon tetrachloride ( $\text{CCl}_4$ ), respectively. Two crystals are grown under identical conditions (growth temperature, growth rate, V/III ratio) and are grown sequentially to minimize any differences between the crystals. The epitaxial layers consist of  $\sim 2 \mu\text{m}$  of  $\text{Al}_{0.6}\text{Ga}_{0.4}\text{As}$ , followed by a  $\sim 500 \text{ \AA}$  GaAs cap-layer. The  $\text{Al}_{0.6}\text{Ga}_{0.4}\text{As}$  is doped  $n \sim 4 \times 10^{17} \text{ cm}^{-3}$  in one crystal, and  $p \sim 9 \times 10^{18} \text{ cm}^{-3}$  in the other, as verified by  $C$ - $V$  and Hall Effect measurements. The composition of the  $\text{Al}_x\text{Ga}_{1-x}\text{As}$  layer has been confirmed to be  $x \approx 0.61$  for both crystals, as measured by double crystal x-ray diffractometry. Thus, both crystals are identical except for the doping of the  $\text{Al}_{0.6}\text{Ga}_{0.4}\text{As}$  layer.

The two crystals are simultaneously oxidized (at dif-

ferent times and temperatures) to avoid any differences in the oxidation conditions. Before oxidation, the GaAs cap-layer is removed by chemical etching ( $\text{H}_2\text{SO}_4\text{:H}_2\text{O}_2\text{:H}_2\text{O}$ , 1:8:80), and the crystals of different dopings are then both placed in an open tube furnace (supplied with  $\text{H}_2\text{O}$  vapor via an  $\text{N}_2$  carrier gas) and oxidized simultaneously. After oxidation, the crystals are cleaved and stained in an  $\text{HCl:H}_2\text{O}_2\text{:H}_2\text{O}$  (1:4:40) solution for imaging in a SEM.

Figure 1 shows SEM images of stained crystal cross sections for (a)  $p$ -type and (b)  $n$ -type samples oxidized simultaneously at 500 °C for 45 min. The oxide is considerably thicker for the (a)  $p$ -type sample ( $x_j \sim 0.6 \mu\text{m}$ ) than for the (b)  $n$ -type sample ( $x_j \sim 0.3 \mu\text{m}$ ). Similar trends [ $x_j(p\text{-type}) > x_j(n\text{-type})$ ] are observed at all temperatures (425–525 °C) and all times (30–75 min) investigated. The discrepancy between the thickness of the  $\text{Al}_{0.6}\text{Ga}_{0.4}\text{As}$  layers in Fig. 1 for the (a)  $p$ -type and (b)  $n$ -type samples is due to etching of the  $\text{Al}_{0.6}\text{Ga}_{0.4}\text{As}$  from the by-products of the  $\text{CCl}_4$  source during the crystal growth.<sup>10</sup>

Figure 2 shows the results of oxidation depth measurements versus time for both (a)  $p$ -type and (b)  $n$ -type samples at 500 °C. The rate for the  $p$ -type sample is significantly higher than that of the  $n$ -type sample. In accordance with classical oxidation theory for sufficiently thick films

116p

FIG. 1. Scanning electron microscope images of stained crystal cross sections of native oxides formed via  $\text{H}_2\text{O}$  vapor oxidation (500 °C, 45 min) from (a)  $p$ -type and (b)  $n$ -type  $\text{Al}_x\text{Ga}_{1-x}\text{As}$  of the same composition ( $x \approx 0.61$ ). The  $p$ -type sample ( $x_j \sim 0.6 \mu\text{m}$ ) oxidizes more rapidly than the  $n$ -type sample ( $x_j \sim 0.3 \mu\text{m}$ ).

<sup>a)</sup>AT&T Doctoral Fellow

<sup>b)</sup>Now at Amoco Technology Company, Amoco Research Center, Naperville, IL 60566

101. 13

HIGH-PERFORMANCE PLANAR NATIVE-OXIDE BURIED-MESA INDEX-GUIDED

AlGaAs-GaAs QUANTUM WELL HETEROSTRUCTURE LASERS

S. J. Caracci, F. A. Kish,<sup>a)</sup> N. Holonyak, Jr., and S. A. Maranowski

Electrical Engineering Research Laboratory

Center for Compound Semiconductor Microelectronics, and

Materials Research Laboratory

University of Illinois at Urbana-Champaign, Urbana, Illinois 61801

S. C. Smith and R. D. Burnham

Amoco Technology Company, Amoco Research Center, Naperville, Illinois 60566

ABSTRACT

High-performance planar "buried-mesa" index-guided AlGaAs-GaAs quantum well heterostructure (QWH) lasers have been fabricated by oxidation ( $H_2O$  vapor +  $N_2$  carrier gas,  $425-525^\circ C$ ) of a significant thickness of the high composition  $Al_xGa_{1-x}As$  upper confining layer (outside the active stripe). The oxide provides excellent current confinement for low-threshold laser operation and a low refractive index ( $n \sim 1.6$ ) for transverse optical confinement and index-guiding. Laser diodes with  $\sim 4 \mu m$ -wide active regions exhibit 300 K continuous (cw) laser thresholds of 8 mA, with single longitudinal mode operation to 23 mW/facet, and maximum output powers of 45 mW/facet (uncoated). Devices fabricated on a lower confinement  $Al_xGa_{1-x}As$ -GaAs QWH crystal ( $x \leq 0.6$  instead of  $x \geq 0.8$ ) with  $\sim 4 \mu m$ -wide active stripes exhibit 300 K cw thresholds of 9 mA and total external differential quantum efficiencies of 66%. Peak output powers  $> 80$  mW/facet (uncoated) with linear L-I characteristics over the entire operating range are observed. In limited "lifetest" these laser diodes have been operated  $> 500$  h without significant degradation.

RESONANCE AND SWITCHING IN A NATIVE-OXIDE-DEFINED  
 $\text{Al}_x\text{Ga}_{1-x}\text{As-GaAs}$  QUANTUM WELL HETEROSTRUCTURE LASER ARRAY

N. El-Zein, N. Holonyak, Jr., and F. A. Kish<sup>a)</sup>

Electrical Engineering Research Laboratory,  
Center for Compound Semiconductor Microelectronics, and  
Materials Research Laboratory

University of Illinois at Urbana-Champaign, Urbana, Illinois 61801

S. C. Smith, J. M. Dallesasse, and R. D. Burnham

Amoco Technology Company, Amoco Research Center, Naperville, Illinois 60566

ABSTRACT

A twin linear-array coupled-cavity  $\text{Al}_x\text{Ga}_{1-x}\text{As-GaAs}$  quantum well heterostructure laser, a stripe-geometry coupled two-dimensional array, is described that, unlike the usual stripe laser, exhibits mode switching and multiple switching in the light power (L) versus current (I) characteristic (L-I) with increasing current.

# Diffusion of manganese in GaAs and its effect on layer disordering in $\text{Al}_x\text{Ga}_{1-x}\text{As}$ -GaAs superlattices

C. H. Wu, K. C. Hsieh, G. E. Höfler, N. EL-Zein, and N. Holonyak, Jr.  
*Center for Compound Semiconductor Microelectronics, Department of Electrical and Computer Engineering and Materials Research Laboratory, University of Illinois at Urbana-Champaign, Illinois 61801*

(Received 8 April 1991; accepted for publication 10 June 1991)

Several diffusion runs of Mn in GaAs are performed in sealed quartz ampoules with four different Mn-containing sources: (a) solid crystal granules of Mn, (b)  $\text{Mn}_3\text{As}$ , (c) MnAs, and (d) Mn thin films coated on GaAs substrates. Among these, only MnAs results in a smooth GaAs surface and uniform doping distributions. For the others interactions between the source materials and GaAs substrates give rise to poor surface morphologies and inhomogeneous distributions of new-phase (Mn,Ga) crystals. For diffusion at 800 °C, surface  $p$ -type carrier concentrations as high as  $10^{20}/\text{cm}^3$  are obtained. Diffusion profiles determined by  $C$ - $V$  techniques resemble those obtained for Zn diffusions. A substitutional-interstitial mechanism is suggested as the primary diffusion mechanism for Mn in GaAs. Data are also presented showing that layer disordering in AlGaAs-GaAs superlattices can be induced by Mn impurities.

Various impurities have long been incorporated into bulk semiconductors or epitaxial layers during crystal growth or processing for various device applications. Zn, Be, and Mg are commonly used for  $p$ -type doping in GaAs-and/or InP-based compound semiconductors grown by metalorganic chemical vapor deposition (MOCVD) or molecular beam epitaxy (MBE), but Cd and Mn are rarely used. With Cd and Mn, it is difficult to dope above  $1 \times 10^{18}/\text{cm}^3$ .<sup>1-3</sup> Additional concern with Mn doping is the poor surface morphology. Ripple-like features parallel to  $[1\bar{1}0]$  are observed in MBE-grown GaAs with Mn doping higher than  $1 \times 10^{17}/\text{cm}^3$ . The origin of the ripple structure has been suggested to be associated with the surface segregation of the doping species during crystal growth.<sup>2</sup> Very limited data on Mn diffusion are available in the literature, and a surface concentration of only  $2 \times 10^{18}/\text{cm}^3$  has been reported by Seltzer.<sup>4</sup> In the present work we report that very high carrier concentrations ( $\sim 10^{20}/\text{cm}^3$ ) from Mn diffusion can be realized with smooth surface morphology. Our results indicate that using different Mn-containing sources for the diffusion of Mn in GaAs can have a profound influence on the ultimate surface carrier concentration, surface morphology, and as a result, on the effectiveness of impurity induced layer disordering (IILD) in AlGaAs-GaAs superlattices.<sup>5</sup>

Four different Mn-containing sources have been used to introduce Mn into GaAs, including separate solid sources of Mn, MnAs, or  $\text{Mn}_3\text{As}$  (granules) enclosed in the quartz diffusion ampoules, as well as thin Mn films that are deposited directly onto the substrates by electron beam evaporation. The substrates for Mn diffusion are semi-insulating GaAs. The undoped AlGaAs-GaAs superlattices investigated here for IILD have been grown by low-pressure metalorganic chemical vapor deposition in an Emcore GS 3100 reactor. The sources for the growth of column III and V materials are trimethylaluminum (TMAI), trimethylgallium (TMGa), and 100%  $\text{AsH}_3$ , respectively. Crystal growth temperatures have been varied from 600 °C for

GaAs layers to 740 °C for AlGaAs layers. The superlattice structure consists of 20 periods of  $\text{Al}_x\text{Ga}_{1-x}\text{As}$  ( $x \sim 0.4$ ) and GaAs, with both wells and barriers approximately 180 Å thick. These layers are confined on top (1000 Å) and on the substrate side (1000 Å) by two  $\text{Al}_y\text{Ga}_{1-y}\text{As}$  ( $y = 0.85$ ) layers. As usual a GaAs buffer layer is grown first, and a GaAs cap layer is grown on top.

Sample preparation for Mn diffusion consists of the usual surface cleaning procedures of degreasing with solvents, followed by an  $\text{NH}_4\text{OH}$  etch for 1 min. The samples are then loaded into degreased and etched quartz ampoules with the Mn sources, and are evacuated to  $\sim 2 \times 10^{-6}$  Torr and sealed. The diffusions are performed at 800 °C for times less than 12 h. Nomarski optical microscopy and transmission electron microscopy (TEM) are used to investigate the surface morphology and annealing surface reactions. Mn diffusion profiles were obtained by either secondary ion mass spectroscopy (SIMS) or capacitance-voltage ( $C$ - $V$ ) electrochemical etch profiler.

The surface morphologies of the samples after Mn-diffusion at 800 °C (2 h) using different Mn-containing sources are shown in Fig. 1. Different degrees of surface degradation of the GaAs surfaces have occurred depending on the choice of Mn sources. Poor surface morphologies result from chemical reactions between the vapor of the Mn-containing sources and GaAs substrates are clearly observed except when MnAs is used as the diffusion source. As a result of these reactions, inhomogeneous new-phase crystals of (Ga, Mn) form across the surface and to various depths as identified by cross-section transmission electron microscopy and energy dispersive x-ray spectroscopy. These numerous minute crystals, having probably a cubic structure, are generally smaller than 500 Å. In addition to the phase transformation near the surface, dislocations and dislocation loops of various densities are observed at different depths in the substrate depending on the diffusion conditions. Detailed data will be presented elsewhere. SIMS profiles obtained at different positions on the Mn-

# EFFECT OF ANNEALING TEMPERATURE ON HOLE CONCENTRATION AND LATTICE RELAXATION OF CARBON DOPED GaAs AND $\text{Al}_x\text{Ga}_{1-x}\text{As}$

G. E. Höfler, H. J. Höfler,<sup>1)</sup> N. Holonyak, Jr. and K. C. Hsieh

Department of Electrical and Computer Engineering and

Center for Compound Semiconductor Microelectronics,

University of Illinois at Urbana-Champaign

208 N. Wright St., Urbana, IL 61801

<sup>1)</sup>Department of Material Science Engineering

University of Illinois

1304 W. Green St, Urbana IL, 61801

## ABSTRACT

Measurements of the hole density in heavily carbon-doped GaAs and  $\text{Al}_x\text{Ga}_{1-x}\text{As}$  as a function of the annealing temperature are presented. It is shown that the hole density increases and the hole mobility decreases after annealing at low temperatures ( $T < 550^\circ\text{C}$ ). However, higher annealing temperatures ( $T > 600^\circ\text{C}$ ) result in a reduction of the hole concentration reaching a maximum carrier concentration of  $\approx 5 \times 10^{19} \text{ cm}^{-3}$ . These changes observed in the electrical properties can be explained by two mechanisms: 1) the passivation of carbon acceptors by hydrogen incorporated during growth; and 2) the change in the lattice site location of carbon atoms, which is dependent on the total carbon concentration.

# JOHN BARDEEN AND THE POINT-CONTACT TRANSISTOR

It is not widely appreciated that Bardeen first recognized minority-carrier injection, which is the basis for the original bipolar transistor and the beginning of modern electronics.

Nick Holonyak Jr

To this day it is not well understood that the bipolar transistor began with John Bardeen and Walter H. Brattain's point-contact transistor.<sup>1</sup> The invention of the point-contact transistor was a momentous event, not only in itself but even more because of the unimaginable revolution in electronics that followed. This revolution, which continues unabated, had a beginning: Bardeen's recognition of minority-carrier injection—that is, his realization that an applied voltage causes valence band holes from the surface region of an n-type semiconductor material near a metal contact to be injected into the bulk of the material. This realization made the semiconductor suddenly important and no longer just an interesting material to study.

The historic recognition of minority-carrier injection was followed a week later by the famous 23 December 1947 demonstration to Bell Telephone Laboratories "brass," as John called them, of transistor amplification and audio operation.

My main purpose in this article is to report largely unknown information from conversations, lectures, seminars, interviews and so on concerning Bardeen's identification, based on his work with Brattain, of minority-carrier injection and his invention with Brattain of the point-contact transistor, the prototype for all succeeding injection devices.

It is worth recalling that in 1947 the state of semiconductor knowledge and technology was, to say the least, primitive. Crystal quality was poor, and it was not even known whether germanium, the original transistor material, was a direct-gap or indirect-gap semiconductor.<sup>2</sup> It was finally determined to be the latter in 1954. This property turned out to be fortuitous in that it gave long enough minority-carrier lifetimes to permit realization of the point-contact transistor, which was the original bipolar transistor.<sup>1,2</sup> Besides starting a revolution in

**Nick Holonyak Jr** is Center of Advanced Study Professor of Electrical and Computer Engineering at the University of Illinois, Urbana-Champaign.